ELECTRON-OPTICAL STUDIES OF THE PHOTOELECTRIC EFFECT

Thesis by

J. H. BRADNER

In Partial Fulfillment of the Requirements

for the Degree of Doctor of Philosophy

California Institute of Technology
Pasadena, California

1941

TABLE OF CONTENTS

I. ABSTRACT

In this laboratory Carl F. J. Overhage, and elsewhere other experimenters, have found that the normal energy distribution of photoelectrons from sodium does not agree with the Fowler-DuBridge theory of surface photo-electric emission. A marked discrepancy occurs. It has been suggested that gas contaminations may produce a cathode barrier which varies in a complicated way over the surface, and that due to this, and different work functions of various crystal faces, cathode areas which are effective in producing emission vary with incident radiation energies. It has been also suggested that the normal energy distribution from a rough surface, i.e., surface elements inclined at angles to the field, may be different from that predicted by the Fowler-DuBridge theory.

An electron-microscope has been constructed for observing the photoelectric emission from a sodium surface. Electron pictures of the emitting surface have been taken for a variety of incident light energies. At the magnification used (10 diameters) no significant difference was observed.

The Fowler theory for emission at $0^{\circ}K$ has been adapted to the case of a rough surface. This modified theory does not predict any altered shape of the normal energy distribution curves when the retarding fields are high although it does predict changes for low fields and for very rough surfaces.

II. INTRODUCTION

In 1937 C.F.J. Overhage[1] published results of measurements in this laboratory on the normal energy distribution of photoelectrons from a sodium surface. His work showed that the experimental curves did not agree with the theoretical predictions of the Fowler-Dubridge[2-4] theory. Figure 2.1* is Overhage's plot of the observed vs. the theoretical distribution at 300°K, the temperature at which his experiments were carried out. Incidentally, there is also plotted the same experimental curve vs. the theoretical curve for 600°K. It will be seen that the fit is better for the higher temperature, but the significance of this is questionable. Other experimenters have reported a similar discrepancy. Hill and Dubridge[5] noted its occurence in total energy distributions, as also did Brady and Jacobsmyer[6]. An investigation by Mann and Dubridge[7] on absolute photoelectric yield indicated that here also theory and experiment were at variance. Henshaw[8], working with thin potassium films, found that most of his experimental curves fit Fowler-Dubridge curves of lower temperatures. Were all these discrepancies due to experimental difficulties, or to an inadequacy of the Fowler-DuBridge theory?

The most commonly suggested[9-11] explanation for the difference between observed and theoretical energy distributions is that gas contaminations are responsible for the altered shapes of the curves. Changes in emission curves with age have actually been observed[12] in experiments where the total cothode emission as a function of frequency is measured in an accelerating field.

---

* C.F.J. Overhage thesis, Fig. 12, p. 78

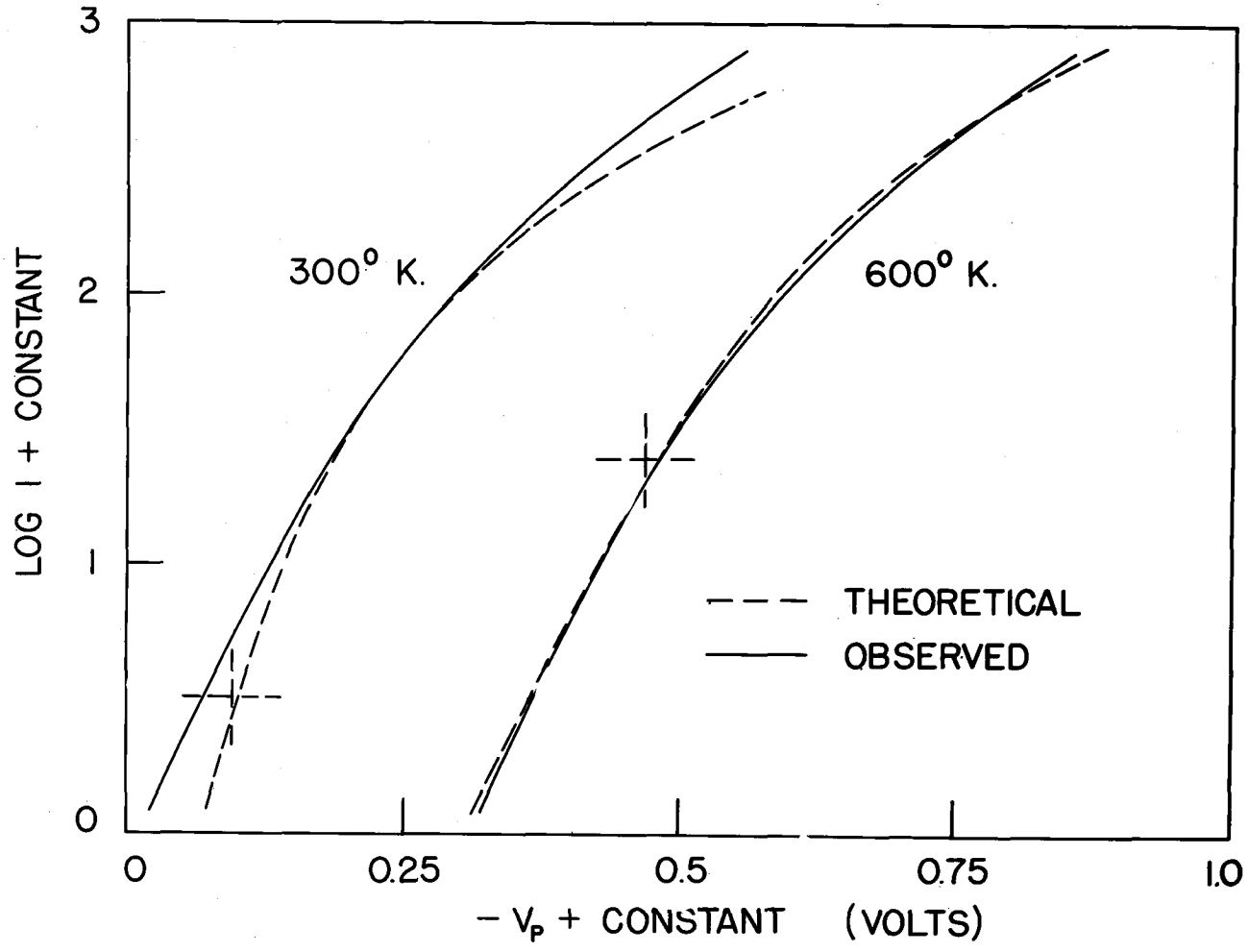
3
2
1
0
LOG I + CONSTANT
300° K.
600° K.
THEORETICAL
OBSERVED
0
0.25
0.5
0.75
1.0
− V_p + CONSTANT (VOLTS)

Fig. 2.1

It sounds reasonable that a contamination would have different work function from that of pure sodium, and hence would have a different (probably higher) photo-electric threshold. One would thus expect that a larger cathode area would emit at higher illumination frequency.

Furthermore, any non-cubic crystals of sodium will have different work functions for the various crystal faces, and hence will begin emission at different energies.

The suggestion that short wave light penetrates through to the backside of small lumps can be discounted. Measurements by Wood[13] show that sodium is transparent only below 2100 Angstroms.

Overhage (loc.cit.) felt that due to the retarding field joined to the cathode potential barrier in his experiment, gas contaminations with their attendant alterations in cathode work function should not affect the transmission of electrons. Houston[14] has shown that under the conditions of Overhage's work, the transmission coefficient is approximately independent of the shape of the cathode potential barrier.

A final possibility was that the rough surface of an evaporated sodium film behaved far differently from the ideally plane surface upon which all previous theoretical treatments had been based.

Houston (loc.cit.), generalizing on the work of Mitchell,[15-16] evolved a quantum-mechanical theory which could be made to fit Overhage's results quite well. However, it still seemed worthwhile to investigate the above possibilities.

With the recent developments in electron optics it appeared that one could construct an apparatus to image by means of photo-electrons

the emission from a sodium cathode; and to actually study the pattern of the emission and its changes with age and with frequency of incident light.

Early in 1938, Dr. Houston began constructing a brass system for preliminary experiments on cathode imaging; and was already busily engaged in leak hunting when in March of 1938 the writer appeared on the scene. By August, fairly satisfactory images (approx. 20 diam magnification) of the emission from an oxide pattern upon a nickel ribbon filament were obtained.

The apparatus was not suitable, however, for photo-electric studies; so in April 1939, a glass-metal apparatus was constructed. After several mutations, there resulted the form which will be described here. Meanwhile, under Dr. Houston's ministrations, the original apparatus became an electron microscope.

III. ELECTRON OPTICS

3.1. Analogy to geometrical light optics

The term electron optics refers to the study of the behavior of electron beams in electrostatic or magnetic fields, especially when the beams are used for the purpose of optical imaging; it is so named in analogy to light optics.

The need of this study was first acutely felt, less than ten years ago, in designing cathode ray tubes, although Sir William Hamilton[17-21] had laid its basis in a series of papers about 1830 with an elaborate analogy between the paths of light beams and charged particles in a conservative field. Wiechart[22] in 1899, and Fleming[23] in 1897 mentioned the focusing action of a magnetic coil. Braun[24] in 1897 used space charge focusing in the well known Braun tube. And in 1908 Westphall[25] used the Wehnelt electrostatic cylinder lenses to produce a focusing beam in his oscilloscope. These experiments, however, were done without realization of the strong analogy between light and electron beams; and the focusing action of fields was not considered from a lens standpoint at all.

In electron optics as in light, one can apply geometrical considerations without appealing to the wave nature of the beams. All of the ordinary lens formulae of geometrical light optics can be built up from the four laws:

1. Rectilinear propagation in free space
2. Law of refraction at a plane surface
3. Law of reflection at a plane surface
4. Independence of the different rays of a beam of light.

The first we know to be true for electrons; and the fourth also, providing the current density is low. It is easy to show in a simple case that the second and third also hold. Consider a plane interface

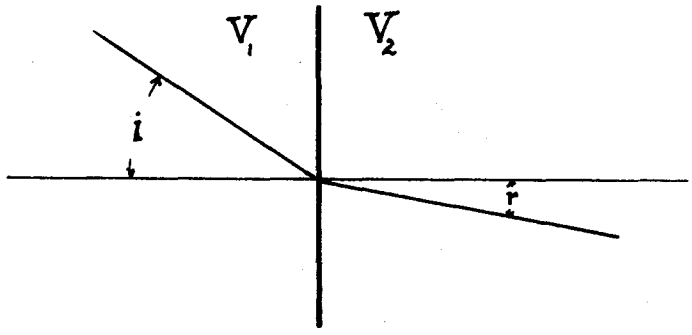

Fig. 3.1

between two potential regions V_1 and V_2 as shown in Figure 3.1, and consider a beam of electrons of velocity v with energy

$$\tfrac{1}{2} m v_1^2 = eV_1 \qquad \ldots\ldots\ldots\ldots (1)$$

incident at an angle i. If V_2 is greater than V_1 the beam crosses the interface, and proceeds with some velocity v_2 at some angle r. The normal component of velocity is changed by the field at the interface while the tangential component remains the same. Thus

$$v_{tan} = v_1 \sin i = v_2 \sin r \qquad \ldots\ldots\ldots\ldots (2)$$

which can be rewritten

$$\frac{\sin i}{\sin r} = \frac{v_2}{v_1} = \frac{\mu_2}{\mu_1} \qquad \ldots\ldots\ldots\ldots (3$$

the familiar Snell's law equation for index of refraction. We can calculate the ratio μ_2/μ_1 of the "indices of electron refraction" of the two media in terms of the potentials V_1 and V_2, since we have (1) and its analogous equation for the region V_2:

$$\frac{\mu_2}{\mu_1} = \frac{v_2}{v_1} = \sqrt{\frac{V_2}{V_1}} \qquad \ldots\ldots\ldots\ldots (4$$

If V_2 is less than V_1 the electron will be deflected back out of the region V_2 into V_1 again, with tangential component unchanged but normal component reversed. Hence it will go off at an angle i' equal to i obeying the ordinary optical law of reflection.

3.2. Analogy in the general case of electrostatic and magnetostatic fields

The analogy between electron beams and light beams can be shown in a much more general way by comparing the principle of least time (Fermat's principle) for light with the principle of least action for electrons.

The principle of least time states that a light ray in any optical system follows the path which takes the shortest time . Now the velocity, v, of light in a medium is related to the index of refraction by the equation

$$\mu = \frac{c}{v} \qquad \ldots\ldots\ldots\ldots (1$$

where c is the velocity of light in vacuum; so that the time to go from some point A to a point B is

$$t = \frac{1}{c} \int_A^B \mu ds \qquad \ldots\ldots\ldots\ldots\ldots\ldots (2)$$

And the usual statement of the variation principle is

$$\delta \int_A^B \mu ds = 0 \qquad \ldots\ldots\ldots\ldots\ldots\ldots (3)$$

The principle of least action* can be written

$$\delta \int_A^B p ds = 0 , \qquad \text{or} \qquad \delta \int_A^B \frac{\partial L}{\partial v} ds = 0 \qquad \ldots\ldots\ldots (4)$$

where p is the scalar magnitude of the momentum and L is the Lagrangian function, which for an electron moving nonrelativistically with velocity v in electric and magnetic fields is*

$$L = \tfrac{1}{2}mv^2 - Ve - \frac{e}{c}(\mathbf{v} \cdot \mathbf{A}) \qquad \ldots\ldots\ldots (5)$$

where V is the electrostatic potential and $\mathbf{A}$ the magnetic vector potential, the left-slanting symbols always refering to vector quantities. Hence by (4)

$$\delta \int_A^B [mv - \frac{e}{vc}(\mathbf{v} \cdot \mathbf{A})] ds = 0 \qquad \ldots\ldots\ldots (6)$$

Comparing with (3), we see that the path of an electron moving with velocity v through electric and magnetic fields is analogous to the path of a ray of light, providing we call the index of refraction for the electron

$$\mu = k [mv - \frac{e}{vc}(\mathbf{v} \cdot \mathbf{A})] \qquad \ldots\ldots\ldots (7)$$

---

* See for instance Webster, Dynamics, Chap.IV, eq'n (9) or Lamb, Higher Mechanics p, 103.

* See for instance Max Born, Mechanics of the Atom, p. 208.

The first term, kv, represents the index of refraction of an electron moving with velocity, v, in electrostatic fields; and since $\frac{1}{2}mv^2 = Ve$ determines the velocity at every point, the index is a function of position in the lens system and is constant over each equipotential. V has no discontinuities; so the index of refraction does not change abruptly as in ordinary optics; and it is as though one had inhomogeneous optical substances.

The second term, containing a scalar product of $\mathbf{v}$ by $\mathbf{A}$, is the part of the index of refraction due to a magnetic field; and depends on both the position and the direction of motion of the electron. The index of refraction due to a magnetic field is thus that of an inhomogeneous anistropic medium.

The analogy of electron beams to light beams implies that one can construct electron lenses and mirrors of axially symmetrical fields. There will be in an electron lens system no abrupt changes of refractive index, rather the analogue of a multitude of lenses of varying indices, with the lens surfaces, in an electrostatic system, corresponding to equipotential surfaces. Fig. (3.2) shows equipotentials (which are surfaces of constant μ) for an electrostatic system of two cylinders as used in cathode ray tubes.

In an ideal lens system it is assumed that rays leaving a point object travel in straight lines until they strike the lens; then they are bent in some manner or other until they leave the lens system and travel again in straight lines to intersect at a point image. The exact point convergence is an idealization; so one normally considers

as an approximation first order, or paraxial, imaging.

Abbes' geometrical treatment, in terms of cardinal points, of first order imaging by light optical lens systems applies regardless of what physical means are used for image formation. It only requires that the light propagate rectilinearly outside the lens system. Specification of the principal planes and focal planes of any lens system completely determines its paraxial focusing action.

A geometrical treatment of electron lens systems in terms of principal planes and focal planes is possible since electrons travel in straight lines outside a lens; and it is frequently of value, although in electrostatic systems the potentials and hence the indices of refraction are different on the two sides of a lens. The treatment is complicated since the nodal points no longer lie in the unit planes. The focal planes F_1 and F_2 and the principal planes H_1 and H_2 for the system of Fig. (3.2) are indicated in Fig. (3.3).

3.3. Motion of electrons in axially symmetric electrostatic fields

The calculation of lens equations requires a knowledge of the electron trajectories. The differential equation governing these trajectories is easily found, but its solution in general can only be approximated. Consider first the electrostatic case of an axially symmetric electrode system, the electrons being emitted with negligible velocities into a region of zero potential. In any region of varying potential, and hence non-zero field, the force urging an electron in any particular direction ξ is given by the product of the

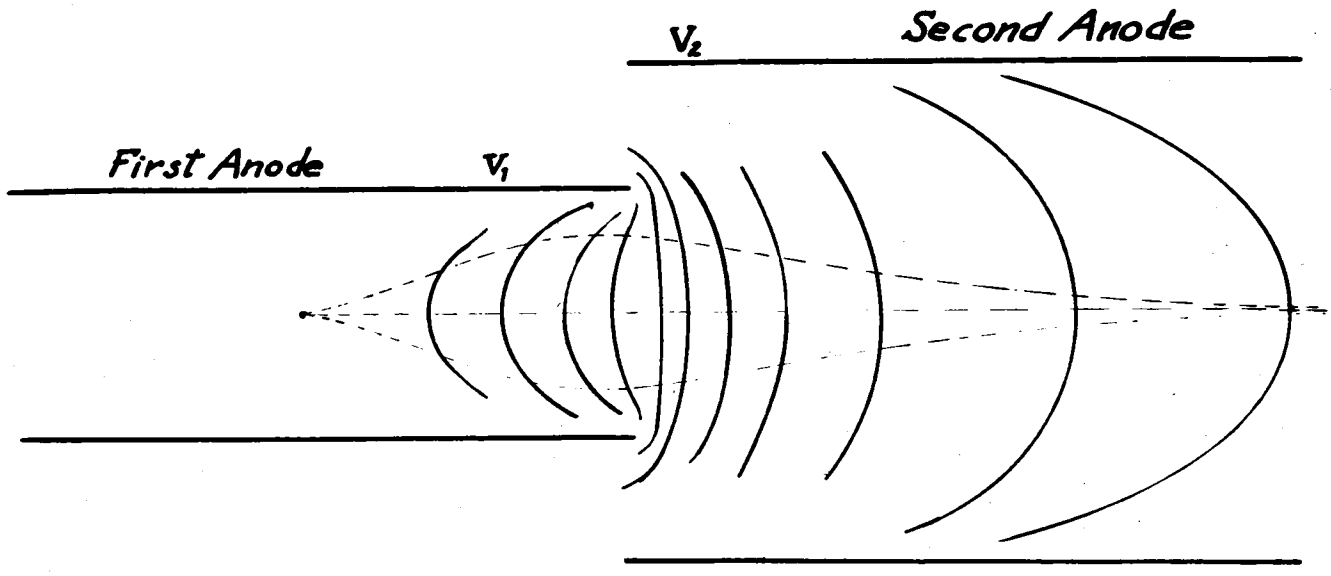

Fig. 3.2

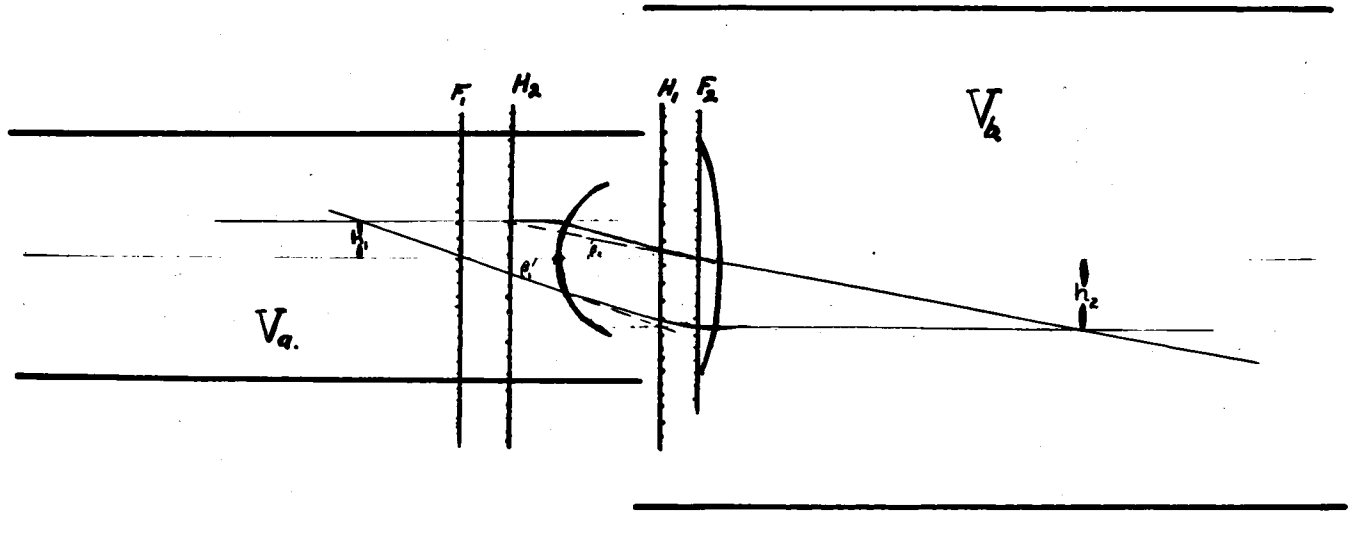

Fig. 3.3

electronic charge by the field in the ξ direction. That is,

$$F_\xi = - eE_\xi = e \frac{\partial V}{\partial \xi} \qquad \text{since} \qquad \ldots\ldots\ldots (1)$$

$$\mathbb{E} = - \nabla V \quad . \qquad \ldots\ldots\ldots (2)$$

The motion of an electron can be described by the cylindrical coordinates r, φ, z; and the nonrelativistic* equations of motion are

$$- E_r e = \frac{\partial V}{\partial r} \; e = m\ddot{r} \qquad \ldots\ldots\ldots (3)$$

$$- E_z e = \frac{\partial V}{\partial z} \; e = m\ddot{z}$$

where the dots represent differentiation with respect to time. There will be no φ-component of motion, since there is no field in that direction, and it is assumed that the electron starts with no velocity.

A first integral is the energy equation

$$\frac{m}{2} \left(\dot{r}^2 + \dot{z}^2\right) = Ve \qquad \ldots\ldots\ldots (4$$

but except in special cases the equations of motion can not be solved further except by series. However they can be put in a somewhat more useful form with time derivatives eliminated, the so-called trajectory equation, which is obtained as follows:

---

* Approximately valid up to 50 K.V. energy electrons.

By calculus

$$\frac{d^2r}{dt^2} = \frac{d}{dt}\left(\frac{dr}{dt}\right) = \frac{d}{dz}\left(\frac{dr}{dz}\frac{dz}{dt}\right)\frac{dz}{dt}$$

$$= \frac{d^2r}{dz^2}\left(\frac{dz}{dt}\right)^2 + \frac{dr}{dz}\frac{d^2z}{dt^2} \qquad \ldots\ldots\ldots(5)$$

In order to eliminate the $\left(\frac{dz}{dt}\right)^2$ term, we rewrite the energy equation (4)

$$\tfrac{1}{2}m\left(\frac{dz}{dt}\right)^2\left[1+\left(\frac{dr}{dz}\right)^2\right] = Ve \qquad \ldots\ldots\ldots(4a)$$

Inserted into (5) this gives

$$\frac{d^2r}{dt^2} = \frac{d^2r}{dz^2}\,\frac{2Ve}{m\left[1+\left(\frac{dr}{dz}\right)\right]} + \frac{d^2z}{dt^2}\frac{dr}{dz} \qquad \ldots\ldots\ldots(6)$$

Using the equations of motion (3), we have

$$\frac{e}{m}\frac{\partial V}{\partial r} = \frac{d^2r}{dz^2}\,2V\frac{e}{m}\,\frac{1}{1+\left(\frac{dr}{dz}\right)^2} + \frac{e}{m}\frac{\partial V}{\partial z}\frac{dr}{dz} \qquad \ldots\ldots\ldots(7)$$

and finally,

$$2V\frac{d^2r}{dz^2} + \left[1+\left(\frac{dr}{dz}\right)^2\right]\frac{\partial V}{\partial z}\,\frac{dr}{dz} - \left[1+\left(\frac{dr}{dz}\right)^2\right]\frac{\partial V}{\partial r} = 0 \qquad \ldots\ldots\ldots(8)$$

Note that this equation is independent of e and m, and is homogeneous in V. Hence one can conclude that the focal lengths and aberrations of electrostatic lenses are independent of the charged particles used, and depend not on actual values, but only on the ratios of voltages of elements of the lens. The equation is also homogeneous in r,z, so that changing all dimensions by the same factor will not affect the lens properties.

The trajectory equation (8) can be further simplified if, as in optics, we consider first order imaging by paraxial rays; and then any deviations from paraxial imaging will be aberrations. (Electron lenses suffer from the same aberrations as light lenses.) To do this we must expand the potential V (r,z) in a series of the form

$$V(r,z) = \sum_{n=0}^{\infty} r^n W_n(z) \qquad \ldots\ldots\ldots\ldots (9)$$

Now V(r,z) satisfies Laplace's equation in cylindrical coordinates,

$$\frac{\partial^2 V}{\partial r^2} + \frac{1}{r}\frac{\partial V}{\partial r} + \frac{\partial^2 V}{\partial z^2} = 0 \qquad \ldots\ldots\ldots\ldots (10)$$

and a solution independent of φ and valid on the axis can be expressed in terms of Bessel's functions of zero order. These functions expand in even powers of r. Hence (9) should contain only even powers of r.

Now

$$\frac{1}{r}\frac{\partial V}{\partial r} = 2W_2(z) + 4r^2 W_4(z) + 6r^6 W_6(z) + \ldots$$

$$\frac{\partial^2 V}{\partial r^2} = 2W_2(z) + 12r^2 W_4(z) + 30r^6 W_6(z) + \ldots \qquad \ldots (9a)$$

$$\frac{\partial^2 V}{\partial z^2} = W_0''(z) + r^2 W_2''(z) + r^4 W_4''(z) + \ldots$$

where the primes represent differentiation with respect to z. Substituting into Laplace's equation (10), and equating coefficients

of equal powers of r to zero we have $W_2(z) = -\frac{1}{2^2} W_o''(z)$

$$W_4(z) = -\frac{1}{4^2} W_2''(z) = \frac{1}{2^2 4^2} W_o^{iv}(z) \quad \ldots\ldots (9b)$$

. . . . . .

By putting $r = 0$, we see $W_0(z) = V_0(z)$, the potential on the axis. So that

$$V(r,z) = V_o(z) - \frac{r^2}{4} V_o''(z) + \frac{r^4}{64} V_o^{iv}(z) + \ldots\ldots \quad \ldots\ldots (11)$$

Putting (11) into the trajectory equation (8), and throwing away terms in r and its powers, we have the equation governing first order imaging,

$$2V_o(z) \frac{d^2 r}{dz^2} + V_o'(z) \frac{dr}{dz} + \frac{V_o''}{2} r = 0 \quad \ldots\ldots (12$$

Except for a few special forms of V(z), this is as far as one can go without recourse to approximate methods, such as are discussed in some detail by Maloff and Epstein [26], or by Myers[27] in his very complete but untrustworthy volume.

3.4 Electrostatic thin lens

In a case of a thin lens, i.e., one in which the strong fields are confined to a small region along the axis compared with the focal length, the focal length can be expressed in terms of an integral in the following way:

Consider that during the passage of an electron through the lens its distance r_o off the axis remains substantially constant.

Make the substitution

$$P = \frac{\sqrt{V_o}}{r_o}\frac{dr}{dz}, \qquad \frac{dP}{dz} = \frac{\sqrt{V_o}}{r_o}\frac{d^2r}{dz^2} + \frac{1}{r_o\sqrt{V_o}}\frac{dr}{dz} \qquad \ldots\ldots (1)$$

in the trajectory equation (12). Then

$$2\sqrt{V_o}\frac{dP}{dz} + \frac{V_o''}{2} = 0 \qquad \ldots\ldots\ldots (2)$$

Dividing by $\sqrt{2V_o}$, and integrating over the lens gives

$$P_B - P_A = \frac{1}{4}\int_A^B \frac{V_o''}{\sqrt{V_o}}\,dz \qquad \ldots\ldots\ldots (3)$$

The principal ray, i.e., the ray which is moving parallel to the axis in the object space, passes through the focal point of the image space. Before entering the lens, $\frac{dr}{dz} = 0$, and hence $P_a = 0$. Upon leaving the lens, $r = r_o$, and $\frac{dr}{dz} = \frac{r_o}{f}$ by geometry, where f is the distance from the lens to the focal point. Hence $P_b = \frac{\sqrt{V_o(B)}}{f}$, and

$$\frac{1}{f} = \frac{1}{4\sqrt{V_o(B)}}\int_A^B \frac{V_o''(z)}{\sqrt{V_o(z)}}\,dz \qquad \ldots\ldots\ldots (4)$$

which can be integrated by parts to give

$$\frac{1}{f} = \frac{1}{8\ V_o(A)}\int_A^B \frac{[V_o'(z)]^2}{[V_o(z)]^{\frac{3}{2}}}\,dz \qquad \ldots\ldots\ldots (5)$$

To go farther, one needs to know $V_o(z)$.

3.5 Motion of electrons in combined electrostatic and magnetic fields.

Gray[28] has transformed the electrostatic equations of motion 3.3 (3) into a series of ordinary differential equations by means of velocity functions; and following Gray, Glaser[29] has done the same thing for combined electrostatic and magnetic fields.

In a magnetic field the φ component of motion is no longer zero, so we must write for the components of acceleration in cylindrical coordinates,*

$$\begin{aligned} v_r &= \dot{r} & a_\rho &= \ddot{r} - r\dot{\varphi}^2 \\ v_z &= \dot{z} & a_z &= \ddot{z} \\ v_\varphi &= r\dot{\varphi} & a_\varphi &= \frac{1}{r}\frac{d}{dt}(r^2\dot{\varphi}) \end{aligned} \qquad \ldots\ldots\ldots (1)$$

The force on an electron moving in a magnetic field is given by

$$F = -e\,[v \times H] \qquad (e \text{ and } H \text{ in e.m.u.}) \qquad \ldots (2)$$

where the field has a vector potential A, given by

$$H = \operatorname{curl} A \;; \qquad \operatorname{div} A = 0 \qquad \ldots (3)$$

The components of the curl in cylindrical coordinates are†

$$H_r = \operatorname{curl}_r A = \frac{1}{r}\left[\frac{\partial A_z}{\partial \varphi} - \frac{\partial r A_\varphi}{\partial z}\right], \qquad H_\varphi = \operatorname{curl}_\varphi A = \left[\frac{\partial A_r}{\partial z} - \frac{\partial A_z}{\partial \rho}\right]$$

$$H_z = \operatorname{curl}_z A = \frac{1}{r}\frac{\partial (r A_\varphi)}{\partial r} - \frac{\partial A_r}{\partial \varphi} \,. \qquad \ldots\ldots (4$$

In case of axial symmetry, A has only a φ- component, so the

† See for instance, Smythe, Static and Dynamic Electricity. McGraw Hill, 1939. (1, 60)

* See for instance Page, Int. to Theor. Ph., § 18.

equations become

$$H_r = -\frac{\partial A_\varphi}{\partial z}$$

$$H_\varphi = 0 \qquad \ldots\ldots\ldots (5)$$

$$H_z = \frac{1}{r}\frac{\partial}{\partial r}(rA_\varphi)$$

Hence from (2), the components of force are

$$F_r = e\dot{\varphi}\frac{\partial}{\partial r}(rA_\varphi)$$

$$F_z = e\dot{\varphi}\frac{\partial}{\partial z}(A_\varphi)$$

$$F_\theta = -e\left[\dot{z}\frac{\partial A_\varphi}{\partial z} + \frac{\dot{r}}{r}\frac{\partial}{\partial r}(rA_\varphi)\right] = -\frac{e}{r}\frac{d}{dt}(rA_\varphi) \qquad \ldots (6)$$

When electrostatic fields are also present, we must add $\frac{\partial V}{\partial r}$ to the right hand side of the first of these equations, and $\frac{\partial V}{\partial z}$ to the right hand side of the second. Then the equations of motion, using (1), are

$$\ddot{r} - r\dot{\varphi}^2 = -\frac{e}{m}\left[\dot{\varphi}\frac{\partial}{\partial r}(rA_\varphi) - \frac{\partial V}{\partial r}\right]$$

$$\ddot{z} = -\frac{e}{m}\left[\dot{\varphi}\frac{\partial}{\partial z}(rA_\varphi) - \frac{\partial V}{\partial z}\right] \qquad \ldots\ldots (7)$$

$$\frac{1}{r}\frac{d}{dt}(r^2\dot{\varphi}) = +\frac{e}{m}\frac{1}{r}\frac{d}{dt}(rA_\varphi)$$

The last equation integrates immediately to give

$$r\dot{\varphi} = \frac{e}{m}A\varphi + C \qquad \ldots\ldots\ldots (8)$$

C can be taken equal to zero since A_φ has an arbitrary zero which can be chosen at the object, where $\dot{\varphi} = 0$. Putting this into (7) gives

$$\ddot{r} = -\frac{e}{m}\left[-\dot{\varphi}A_\varphi + \dot{\varphi}\frac{\partial}{\partial r}(rA_\varphi) - \frac{\partial V}{\partial r}\right]$$

$$= \frac{e}{m}\frac{\partial}{\partial r}\left[V - \frac{1}{2}\frac{e}{m}A_\varphi^2\right] \equiv \frac{e}{m}\frac{\partial Q}{\partial r} \qquad \ldots\ldots (9)$$

and

$$\ddot{z} = \frac{e}{m} \frac{\partial}{\partial z}\left[V - \frac{1}{2}\frac{e}{m} A_\varphi^2\right] \equiv \frac{e}{m} \frac{\partial Q}{\partial z} \qquad \ldots\ldots\ldots \quad (9)$$

where Q is an abbreviation for the terms in the bracket. These are the equations of motion of an electron in combined electrostatic and magnetic fields. Usually one is not interested in the φ-component of motion, for it merely rotates the beam. Note the formal similarity to the electrostatic equations of motion, 3.3 (3).

We will want to express Q as a series in powers of r. To do this, we need the expansion 3.3 (9) for V,

$$V = V_0(z) - \frac{r^2}{4} V_0''(z) + \frac{r^4}{64} V_0^{iv}(z) + \ldots \qquad 3.3.(9)$$

and a similar one for A_φ

$$A_\varphi = \Sigma\, r^n\, G_n(z) \qquad \ldots\ldots\ldots \quad (10$$

Only odd powers will occur, since* A_φ is independent of φ and the solution to the differential equation for $\mathbf{A}$ can be expressed in terms of $J_1(kr) \sim r^{2n+1}$ Substituting the expansion into the differential equation* for $\mathbf{A}$

$$\frac{1}{r}\frac{\partial A_\varphi}{\partial r} + \frac{\partial^2 A_\varphi}{\partial r^2} + \frac{\partial^2 A_\varphi}{\partial z^2} - \frac{A_\varphi}{r^2} = 0 \qquad \ldots\ldots\ldots \quad (11)$$

and equating powers of r as in the electrostatic case, we get

$$A_\varphi = \frac{r}{2} H(z) - \frac{r^2}{16} H''(z) + \ldots\ldots \qquad \ldots\ldots\ldots \quad (12)$$

Hence the expansion for Q is

---

* Cf. e.g. Smythe, Stat. and Dyn. Elect. (Edward's Bros. 1935) eq. 7.021

$$Q = \frac{e}{m}[V(r,z) - \frac{e}{2m}A^2_\varphi] = Q_0(z) - \frac{r^2}{2}Q_2(z) + \frac{r^4}{8}Q_4(z) + \ldots \quad \ldots (13)$$

where

$$Q_0 = \frac{e}{m}V_0 \quad ; \quad Q_2 = \frac{e}{2m}(V'' + \frac{e}{2m}H^2) \quad ; \quad Q_4 = \frac{e}{8m}(V^{iv} + \frac{e}{2m}HH') \quad \ldots (14)$$

Q plays the same role in these equations that V played in the electrostatic case.

Now, the next step will be to, define two velocity functions $u(r,z)$ and $w(r,z)$ subject to only the restrictions

$$\frac{\partial u}{\partial z} - \frac{\partial w}{\partial r} = 0 \quad ; \quad u^2 + w^2 = 2Q \quad \ldots (15$$

It will be seen that

$$u = \dot{r}, \qquad w = \dot{z} \quad \ldots (16$$

satisfy the equations (9), for

$$\ddot{r} = \frac{\partial u}{\partial r}u + \frac{\partial u}{\partial z}w = \frac{\partial u}{\partial r}u + \frac{\partial w}{\partial r}w = \frac{1}{2}\frac{\partial}{\partial r}(u^2 + w^2) = \frac{\partial Q}{\partial r}$$

$$\ddot{z} = \frac{\partial w}{\partial r}u + \frac{\partial w}{\partial z}w = \frac{\partial u}{\partial z}u + \frac{\partial w}{\partial z}w = \frac{1}{2}\frac{\partial}{\partial z}(u^2 + w^2) = \frac{\partial Q}{\partial z} \quad \ldots (17$$

We will express solutions of the velocity functions as power series in r. U will be an odd function, and W an even function of r. Grey explains this choice as follows: "The above powers of r are the ones required in a system symmetrical about the Z axis. In such a system r reverses in sign with $\dot{r}$ and the u series is odd; z does not reverse sign with r and the w- series is even. Aside from such reasoning, the choice of the two series is justified provided they lead to solutions of the differential equation in a form suitable for the purposes of electron-optics."

It can readily be seen from (15) that u & w have opposite parity. The abcve remarks regarding change in sign with r (in cylindrical coordinates) are not clear to Dr. Houston or the writer, and they feel that some further justification is needed.

$$u = ru_1(z) + r^3u_3(z) + \ldots \qquad w = w_0(z) + r^2w_2(z) + \ldots \quad . \; . \; (18)$$

Putting (18) into (15), and using the expansion (13) for Q, there results

$$u_1' = 2w_2 \; ; \qquad u_3' = 4w_4 \; ; \qquad u_5' = 6w_6 \quad . \; . \; . \; . \; . \; . \; (19)$$

$$w_0 = \sqrt{2Q_0} \; : \; u_1^2 + 2w_0w_2 = -Q_2 \; : \; 2w_0w_4 + 2u_1u_2 + w_2^2 = \frac{1}{4}Q_4 \quad . \; . \; . \; (20)$$

This gives a series of ordinary differential equations for the coefficients of the u-series.

$$\sqrt{2Q_0}\, u_1' + u_1^2 = -Q_2 \quad . \; . \; . \; . \; . \; . \; . \; (21)$$

$$\sqrt{2Q_0}\, u_3' + 4u_1u_2 = \frac{1}{2}Q_4 - \frac{u_1'^2}{2} \quad . \; . \; . \; . \; . \; . \; . \; (22)$$

. . . . . .

Thus the equations of motion are reduced to a series of ordinary differential equations, the first of which (a Riccati equation) applies to paraxial imaging, and the rest to higher order aberrations.

The instantaneous focal distance, S_B from any part of the lens can be easily calculated in terms of the coefficients in the above series.

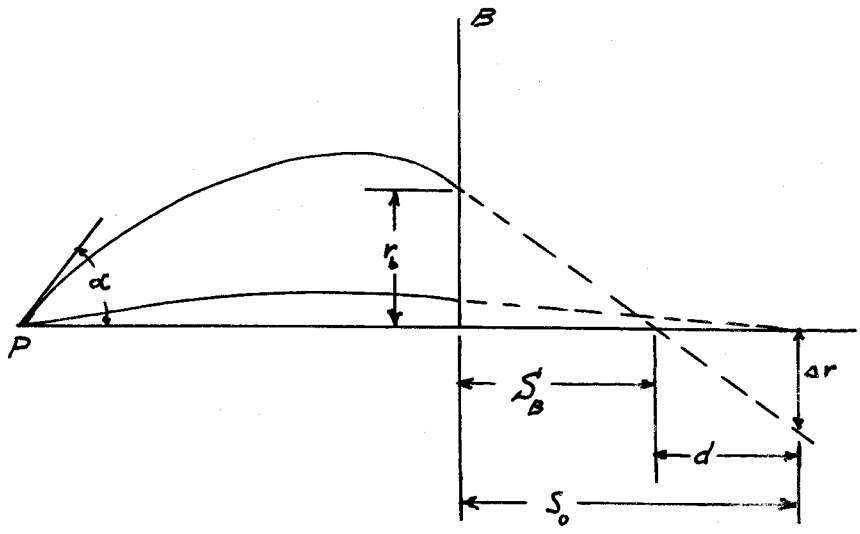

Fig. 3.5

Consider a beam which has left the axis at an angle α at some point P (Fig.3.5) and been deflected by the fields in some manner or other, so that at a plane, z = B beyond which the fields are substantially zero it is travelling in the direction shown by the dotted line. Call the distance S_B the instantaneous focal distance for an electron distant r_B from the axis at the plane B. From the geometry of the figure it is seen that

$$\frac{1}{S_B} = -\frac{r'_B}{r_B} = -\frac{u}{w}\frac{1}{r_B} = -\frac{u_1 + u_3 r_B^2 + u_5 r_B^4 + \cdots\cdots\cdots}{\sqrt{2Q_o} + \frac{1}{2}u'_1 r_B^2 + \frac{1}{4}u'_3 r_B^4 + \cdots\cdots} \quad \cdots\cdots (23)$$

where r'_B is the slope of the trajectory at z = B, and u and w are $\frac{dr}{dt}$ and $\frac{dz}{dt}$. Hence for paraxial rays,

$$\frac{1}{S_{B_o}} = -\frac{u_1(z_B)}{\sqrt{2Q_o(z_B)}} \quad \cdots\cdots (24)$$

where u_1 is given by (21)

3.6. Thin lens of combined electrostatic and magnetic fields.

For paraxial rays 3.5 (23) becomes

$$u_1 = \frac{r'(z)}{r(z)} \sqrt{2Q_0(z)} \qquad \ldots\ldots\ldots (1)$$

and

$$u_2' = \frac{r''}{r} \sqrt{2Q_0} + \frac{r'Q_0'}{r\sqrt{2Q_0}} - \frac{(r')^2}{r^2} \sqrt{2Q_0} \qquad \ldots\ldots\ldots (2)$$

substituting into 3.5 (21) gives

$$r'' + \frac{Q_0'}{2Q_0} r' + \frac{Q_2}{2Q_0} r = 0 \qquad \ldots\ldots\ldots (3)$$

or

$$\sqrt{Q_0} \frac{d}{dz}(r'\sqrt{Q_0}) + \frac{Q_2 r}{2} = 0 \qquad \ldots\ldots\ldots (4)$$

Then if we consider that the strong field extends only the short distance from a point z_0 to a point z_1, we can form the integral

$$r'\sqrt{Q_0} = -\int \frac{Q_2 r}{2\sqrt{Q_0}}\, dz \qquad \ldots\ldots\ldots (5)$$

Since the lens is thin, r can be considered constant over the range of integration, and hence can be taken outside the integral sign. Now $-\frac{r'}{r} = \frac{1}{S}$. Hence

$$\frac{1}{S_0} - \frac{1}{S_1} = \frac{1}{2\sqrt{Q_0}} \int_{z_0}^{z_1} \frac{Q_2(z)}{\sqrt{Q_0(z)}}\, dz \qquad \ldots\ldots\ldots (6)$$

If we consider the principal ray, i.e., the one which enters the lens with $r_0' = 0$, then $\frac{1}{S_1}$ is the reciprocal focal length, and the equation for focal length of a thin lens is

$$\frac{1}{F} = \frac{-1}{2\sqrt{Q_0(z_1)}} \int_{z_0}^{z_1} \frac{Q_2(z)}{\sqrt{Q_0(z)}}\, dz \qquad \ldots\ldots\ldots (7)$$

Inserting the defining equations 3.5 (14), for Q_0 and Q_2, we get

agreement with equation 3.4 (4) when H is zero. When the lens is purely magnetic, i.e., V = constant, the focal length becomes

$$\frac{1}{F} = -\frac{e}{8mV_o}\int_{z_o}^{z_1} H^2 dz \qquad \ldots\ldots\ldots (8)$$

3.7. Spherical Aberration of electron lenses.

Referring to fig. 3.5, the second order terms of 3.5 (23) give

$$d = S_{B_o} - S_B = \frac{\sqrt{2Q_o(z_B)} + \frac{1}{2}u_1'(z_B)r_B^2}{u_1(z_B) + u_3(z_B)\, r_B^2} - \frac{\sqrt{2Q_o(z_B)}}{u_1(z_B)}$$

$$= S_B r_B^2 \left[\frac{\frac{1}{2}u_{1B}u'_{3B} - u_{3B}\sqrt{2Q_o}_B}{u_{3B}\sqrt{2Q_o}_B + \frac{1}{2}u_{1_B}u'_{1B}r_B^2}\right]$$

$$\approx S_B r_B^2 \left[\frac{u_{3B}}{u_{1B}} - \frac{u'_{1B}}{2\sqrt{2Q_o}_B}\right] \qquad \ldots\ldots\ldots (1)$$

or

$$\Delta r = \left[\frac{u_{3B}}{u_{1B}} - \frac{u'_{1B}}{2\sqrt{2Q_o}_B}\right]$$

where u_{3B} is the solution to 3.5 (22) at $z = z_B$. We wish to find u_{1B}, u_{3B}, and u'_{1B} to insert into this equation.

As in the previous section, let r(z) be defined by

$$u_1(z) = \frac{r'(z)}{r(z)}\sqrt{2Q_o(z)} \qquad \ldots\ldots\ldots (2)$$

Then 3.5 (22) becomes

$$u_3' + 4u_3\frac{r'}{r} = \frac{Q_4}{2\sqrt{2Q_0}} - \frac{1}{4Q_0\sqrt{2Q_0}}\left[Q_2 + 2Q_0\left(\frac{r'}{r}\right)^2\right] \quad \ldots\ldots (3)$$

whose solution is

$$u_3(z) = r^{-4}\int_{z_0}^{z}\left\{\frac{Q_4}{2\sqrt{2Q_0}} - \frac{1}{4Q_0\sqrt{2Q_0}}\left[Q_2 + 2Q_0\left(\frac{r'}{r}\right)^2\right]^2\right\} r^4 dz \quad \ldots (4)$$

as can be seen by differentiating (4) to obtain (3) again. Hence

$$u_3(z_B) = r_B^{-4}\int_{z_0}^{z_B}\left\{\frac{Q_4}{2\sqrt{2Q_0}} - \frac{1}{4Q_0\sqrt{2Q_0}}\left[Q_0 + 2Q_0\left(\frac{r'}{r}\right)^2\right]^2\right\} r^4 dz$$

Now by calling

$$\frac{r}{r_B} = h \quad , \text{ so that } \quad \frac{r'}{r} = \frac{h'}{h} \quad , \text{ and } \frac{r_B'}{r_B} = h_B' \quad \ldots\ldots (5)$$

(4) can be rewritten with the aid of 3.5 (21)

$$\sqrt{2Q_{0_B}}u_{1_B}' + u_{1_B}^2 = -Q_{2_B} = 0 \quad \ldots\ldots$$

since it is assumed that the fields are zero at, and beyond, z = B.

We get

$$\Delta r = \frac{r_B^3}{h_B'\sqrt{2Q_{0_B}}}\left[\int_{z_0}^{z_B}\left\{\frac{1}{2\sqrt{2Q_0}}\left(Q_4 - \frac{Q_2^2}{2Q_0}\right)h^4 - \frac{Q_2}{\sqrt{2Q_0}}h^2h'^2 - \tfrac{1}{2}\sqrt{2Q_0}h'^4\right\}dz + \tfrac{1}{2}\sqrt{2Q_{0_B}}\,h'^3_B\right] \quad \ldots\ldots (6)$$

The term standing alone can be included in the integral if we integrate to the image point z_1, instead of to z_B; for since Q_4 and Q_2 are zero beyond z_B, the integrand is a constant equal to $\frac{-2Q_0}{2}h'^4$. And since the electron is traveling in a straight line beyond B, $r_B' = \frac{r_B}{z_1 - z_B}$ so that $z_1 - z_B = \frac{1}{h'_B}$. Thus this extension of the integral just serves to eliminate the term $\frac{1}{2}\sqrt{2Q_{0B}}h'^3_B$. With the abbreviations L, M, and N

one can then write

$$\Delta r = \frac{r_B^3}{h'_B \sqrt{V_o}_B} \int_{z_o}^{z_1} (Lh^4 + 2Mh^2h'^2 + Nh'^4)\, dz \qquad \ldots\ldots (7)$$

where

$$N = \tfrac{1}{2}\sqrt{V_o}$$

$$L = \frac{1}{32\sqrt{V_o}}\left[\frac{1}{V_o}\left(V'' + \frac{e}{2m}H^2\right)^2 - \frac{2e}{m}HH' - V^{iv}\right] \qquad \ldots (8)$$

$$M = \frac{1}{8\sqrt{V_o}}\left[V'' + \frac{e}{2m}H^2\right]$$

We can express (7) in terms of the numerical aperture α, instead of r_B if we multiply and divide by h'^4_o. Then $\alpha = r'_o = r_B h'(z_o)$ and with the help of the equation for magnification,

$$\beta = \frac{h'(z_o)\sqrt{V(z_o)}}{h'(z_1)\sqrt{V(z_1)}} \qquad \ldots\ldots\ldots (9)$$

we get the desired equation for radius of the spurious image due to spherical aberration of an electron lens,

$$\delta = \frac{\Delta r}{\beta} = \frac{\alpha^3}{V(z_o)} \int_{z_o}^{z_1} (Lh^4 + 2Mh^2h'^2 + Nh'^4)\, dz \qquad \ldots\ldots (10)$$

In case of pure magnetic focusing, (10) becomes

$$\delta = \frac{\alpha^3 e}{16mV} \int_{z_o}^{z_1} \left[\left(\frac{e}{8mV}H^4 - HH''\right)h^4 + 2H^2h^2h'^2 - \frac{8m}{e}Vh'^4\right] dz \qquad \ldots (11)$$

where $h'' = \frac{eh}{8mV}H^2(z)$ and is zero at z_o and z_1

By partial integration of (11), using (12), one gets finally

$$\delta = \frac{\Delta r}{\beta} = \frac{\alpha^3 e}{96mV} \int_{z_o}^{z_1} \left(\frac{2e}{mV}H^4 + 5H'^2 - HH''\right)h^4\, dz \qquad \ldots\ldots (13)$$

as the size of the spurious image of a magnetic lens. $H = H(z)$ is the axial z-component of the magnetic field; and $n(z)$ is the ray thru $h(z_0) = 0$ with slope $h'(z_0) = 1$.

3.8 Reduction of Spherical Aberration

The most serious limitation to the resolving power of electron microscopes today lies in the spherical aberration of the magnetic lenses. The usual procedure has been to form a highly concentrated field, and to stop down the lens to a N.A. of approximately 1/100. It will be seen from 3.7 (13) that the spurious image varies as the cube of the numerical aperture α. However, due to the wave properties of electron beams the ordinary equation for resolving power holds:

$$\text{Resolving power} = \frac{\lambda}{2\alpha}$$

The balance of these two factors, aberration vs resolving power, is according to Marton, about 10 A^0 in the present R.C.A. electron microscope.

Scherzer[30] showed that the spherical aberration of a space-charge free electron lens is all of one sign. Rebsch[31] later showed that the aberration could be theoretically made as small as desired by having the magnetic or electric fields very strong in the neighborhood of the object. The length of the field must be made

very small; for the length limits the perfection of the lens. By investigating some magnetic and electric fields which approximated aberration free lenses, Rebsch,[31] and Scherzer[32] concluded that the lower limit of aberration for any practical lens is of the order of magnitude $\delta \approx \frac{f}{4}\alpha^3$. M.v. Ardenne[33] indicates that present electron microscopes have lens error of at least ten times this value.

Glaser[29] points out that generalization upon these specific fields may not be justified, since from the equation 3.7 (13) it appears that one could construct a completely spherical aberration free magnetic lens provided he could obtain a focusing field which satisfied the equation

$$\frac{2e}{mV} H^4 + 5H'^2 - H''H = 0 \quad . \qquad \ldots\ldots\ldots (1)$$

Substitute

$$y = H/H_0 \; ; \quad x = z/l \; ; \quad l = \frac{1}{H_0}\sqrt{\frac{mV}{2e}} \; ; \quad \text{where } H_0 \text{ is the field at } z = z_0 \quad \ldots (2)$$

This puts (1) in the form

$$yy'' = 5y' + y^4 \qquad \ldots\ldots\ldots (3)$$

where now the primes mean differentiation with respect to x, (3) can be rewritten

$$\frac{d}{dx}\left(\frac{y'}{y^5}\right) = \frac{1}{y^2} \qquad \ldots\ldots\ldots (4)$$

and upon multiplying by $\frac{y'}{y^5}$ this integrates to

$$\left(\frac{y'}{y^5}\right)^2 = A - \frac{1}{3y^6} \qquad \ldots\ldots\ldots (5)$$

For $Z = o$, and hence $x = o$, $H = H_0$ so that $y = 1$. Therefore

$A = y_0'^2 + \frac{1}{3}$, and

$$x = \sqrt{3} \int_1^y \frac{dy}{y^2 \sqrt{(3y_0' + 1)y^6 - 1}} \quad \ldots\ldots (6)$$

Putting

$$\alpha = y \sqrt[6]{3y_0'^2 + 1}, \qquad \alpha_0 = \sqrt[6]{3y_0'^2 + 1} \quad \ldots\ldots (7)$$

and reinserting the transformations (2) we have

$$z = \sqrt{\frac{mV/2e}{H_0}}\, \alpha_0 \sqrt{3} \int_\alpha^{\alpha_0} \frac{d\alpha}{\alpha^2 \sqrt{\alpha^6 - 1}} \quad \ldots\ldots (8)$$

where

$$\alpha = \alpha_0 \frac{H}{H_0} \; ; \qquad \alpha_0 = \sqrt[6]{\frac{3mV}{2eH_0^2} \left(\frac{H_0'}{H_0}\right)^2 + 1} \qquad 1 \leq \alpha \leq \alpha_0 \quad \ldots (9)$$

The integral (8) can be evaluated in the form

$$z = \alpha_0 [G(\alpha) - G(\alpha_0)] \quad \ldots\ldots (10)$$

where G (α) can be expressed in terms of elliptic integrals.

Put

$$\frac{1}{\alpha^2} = 1 + \sqrt{3} \frac{\cos\varphi - 1}{\cos\varphi + 1} , \qquad \Delta = \sqrt{1 - k^2 \sin^2\varphi}$$

$$k^2 = \frac{2 + \sqrt{3}}{4} = \sin^2 75^\circ \quad \ldots\ldots (11)$$

$$G(\alpha) = \frac{1}{2\sqrt[4]{3}} \int \frac{d\varphi}{\Delta} + \frac{1}{2} \sqrt[4]{3} \int \frac{\cos\varphi - 1}{\cos\varphi + 1} \frac{d\varphi}{\Delta} \quad \ldots\ldots (12)$$

The first term is an elliptic integral E of the first kind.

Multiplying the second term above and below by $\cos\varphi - 1$, we have

$$\int \frac{\cos\varphi - 1}{\cos\varphi + 1} \frac{d\varphi}{\Delta} = - \int \frac{d\varphi}{\Delta} - 2 \frac{d(\cot\varphi)}{\Delta} + 2 \int \frac{d(\sin\varphi)}{\Delta \sin^2\varphi} \quad \ldots\ldots (13)$$

Partial integration gives

$$\frac{d\varphi}{\Delta} - \frac{2\Delta}{\sin\varphi} + \frac{2\cot\varphi}{\Delta} + 2(F - E) + \frac{2k^2 \sin\varphi\cos\varphi}{\Delta} \quad \ldots\ldots (14)$$

Hence (12) becomes

$$G(\alpha) = \sqrt[4]{3}\,[\Delta \tan\frac{\varphi}{2} - E + \tfrac{1}{2}(1 - \frac{1}{\sqrt{3}})F] \quad \ldots\ldots\ldots (15)$$

Rebsch[34] has shown that the fields which Glaser calculates will not be strong enough to bring a divergent electron beam to focus; however it is possible that there exists some other solution which will make the integral 3.7 (13) zero and will be strong enough to focus electron beams. One can for instance calculate other fields by partial integration of 3.7 (13) and setting the integrands equal to zero.

3.9 Determination of axial potential distribution.

In general the form of V(Z), or H(Z), and the axial derivatives can not easily be given analytically, so they are often experimentally determined.

Electrostatic potentials of axially symetric systems can be measured with considerable accuracy in an electrolytic trough*, wherein is placed an enlarged section model of the lens system, just covered with water. The portions of the lens are connected to a 500 cycle voltage source to correspond to the desired potentials of the lens. Then by means of a bridge and headphones or galvanometer, or a cathode ray tube, the voltage on a probe just under the surface of the water is measured; and by using a pantagraph the equipotentials can be plotted.

---

* See for instance Myers[27] p. 129 ff.

Garbor[36] and later Langmuir[36] have constructed machines to plot electron trajectories directly from an electrolytic trough model. Since the radius of curvature of an electron trajectory is given by

$$R = \frac{2V}{E_n} \qquad \ldots\ldots\ldots (1)$$

where E_n is the field perpendicular to the path, if a small cart is built and the steering wheel so controlled that it turns with this radius, a scriber on the cart will trace out the actual electron trajectory.

An approximate method of calculating potential distribution has been worked out by Dr. Houston, following a paper by Shortley[37]. In it, one plots the cross-section of the electrode system on log scale, with the axis corresponding to log $0 = -\infty$. Then one divides the area between electrodes in the log plot by a number of equally spaced points in the direction of both axes. If one assigns an arbitrary potential to each point he can then progressively correct these potentials. Thus a corrected potential for say the point in the 1 th column, 3 rd row is

$$V_{1_3} = \frac{V_{1_4} + V_{1_2} + e^{2\rho_3}\,(Vk_3 + V_{m_3})}{2(1 + e^{2\rho_3})}$$

where ρ_3 refers to the ordinate in the log graph of the 3-row. One then uses this value to correct V_{m3}, and so on. The entire process is repeated until a stable situation is reached. The rapidity of convergence of correction varies inversely with the number of points taken.

Magnetostatic fields are determined by analogy to the electrostatic fields for the same electrode configuration as the pole-pieces, providing the magnetic fields are not so high that the pole pieces are saturated. For fields of 1000 gauss or more one can use a bismuth spiral. In any case, a jerk out coil attached to a ballistic galvanometer will measure the integral of H; and by starting the coil at various points along the axis within the field, H(Z) can be plotted.

3.10 Wave nature of electron beams.

Thus far in section III it has not been necessary to mention the fact that electrons do, under certain conditions, evidence wave properties. The lens equations here developed would be valid if electron beams showed no such properties; they are in fact satisfactory only when one deals with objects large compared with the wave length.

The wave nature of electron beams as shown by electron diffraction experiments is too familiar to warrant discussion; but a calculation of the wave lengths of the beams commonly used in electron optics will not be out of place.

With a beam of electrons is associated the DeBroglie wave length, λ given by

$$\lambda = \frac{h}{mv} \qquad \ldots\ldots\ldots (1)$$

The energy equation of an electron in potential region V is

$$Ve = \tfrac{1}{2} mv^2 = \frac{1}{2m}(mv)^2 \qquad \ldots\ldots (2)$$

Hence

$$\lambda = \frac{h}{\sqrt{2Vem}} \qquad \ldots\ldots (3)$$

which gives upon putting in the values of e, m, and h for electrons,

$$\lambda(\text{Angstroms}) = \sqrt{\frac{150}{V(\text{volts})}} \qquad \ldots\ldots (4)$$

Hence a 150 volt energy electron has a wave length of $1A^{\circ}$, i.e., about 3/10,000 that of visible light. Efficiency of fluorescent viewing screens, and distance of penetration through matter, demand the use of a kilovolt or more for most electron optical applications, and hence a wave length of less than $0.4A^{\circ}$.

3.11 Advantages of electron beams as compared with light beams*

A list of the more important differences between light and electron beams will be of value in design of optical apparatus, and is herewith presented.

The most obvious advantage possessed by electron beams is their short wave length; for the limit of resolution of an optical

---

* Thanks to F. Zwicky for bringing the writer's attention to this idea in a clear form.

instrument is approximately equal to wave length of illumination used. If then one could construct well-corrected electron lenses, it should be possible to resolve objects with less than an Angstrom separation. Difficulties of construction may limit resolution to a much higher figure, but already electron miscroscopes have pushed the lower limit of "visibility" down to 50A°, almost two orders of magnitude better than attainable with light microscopes.

A second obvious difference between light and electron optics -- and in experiments of the nature detailed in this paper, the electrons have an incontrovertible advantage -- is in studying the emission from a surface. The electron emission gives some information concerning crystal orientations and surface contaminations which can not be detected by light.

Brüche and Johanson seem to have been the first to study the recrystallization of a hot surface, both with a thin tungsten strip and with a platinum-rhodium strip, which were used as hot emitting filaments, Recently several articles have appeared in the Phys. Rev. and elsewhere on investigation of small crystals by cold emission. The process of activation and poisoning of thoriated and oxide coated filaments has been studied by Brüche and Johanson, and others,(40-43). The crystal structure of metal surfaces activated with barium azide or with strontium carbonate(44) was investigated as early as 1933. In all these experiments it was possible to see surface effects which would be very difficult or impossible to observe by ordinary optical methods.

Due to the fact that electron beams are focused by electric and magnetic fields rather than by matter there is no partial absorption

or reflection of energy by lenses. Electrostatic and magnetic fields can be completely superimposed, so that one has two lenses simultaneously in exactly the same place. A much greater range of refractive indices is possible with electron lenses. Furthermore, the focal length of a magnetic lens can be altered through wide ranges merely by changing the magnet current.

Of importance also is the possibility with electric circuits of adding, subtracting, or multiplying the intensities of parts or the whole of an image. Under this head comes the electron multiplier. Here also would be considered a transformer-fed video amplifier, which would suppress the intense image of the sun, but leave its corona bright.

The low inertia and rapid response of electron beam deflecting mechanisms is of importance in oscilloscopes; and Dr. Zwicky has mentioned image stabilization of astronomical images by virtue of this property.

Finally, the fact that electrons are scattered according to the mass of matter passed through, rather than index of refraction, may be of service in electron microscope investigations.

IV. THE PHOTOELECTRIC EFFECT

(1) Theories of the photoelectric effect.

One of the first requirements in establishing a theory of photoelectric phenomena is the choice of a good metal model. In 1916, Millikan[35] determined that the photoelectric process affects the conduction electrons, i.e., the "free" electrons released when the metal crystals are formed. That these electrons formed an electron gas, similar to ordinary gases, had been postulated by H. A. Lorentz who assumed that the electrons are in thermal equilibrium with the lattice atoms, and that they have Maxwellian distribution. In order to hold the electrons within the metal it was necessary to postulate a potential barier at the surface of the metal. Lorentz' model predicted fairly nearly correct values for electrical conduction, and thermionic emission; but it gave a value nearly two times too large for specific heat of the metal.

With the application of quantum mechanics, the Maxwell distribution was altered to the Fermi distribution; and Sommerfeld, Pauli, and others obtained very satisfactory results for the above phenomena. The potential inside the metal is considered to be a three-dimensional array of potential minima, the minima corresponding to the crystal atoms. Near the surface of the metal, the potential rises in the form of a barier and becomes asymptotic to an arbitrary zero outside the metal. Often the barrier is considered discontinuous, as in fig.4.2a. For most calculations the non-uniformity of the potential within the metal can be ignored; and the electron energies are distributed according

to the Fermi-Dirac statistics. The number of electrons having velocity components ξ, η, ζ in the range $d\xi d\eta d\zeta$ is

$$N(\xi\eta\zeta)\, d\xi d\eta d\zeta = \frac{\frac{2m^3}{h^2}}{e^{(\varepsilon-\mu)/kT}+1} \qquad \ldots\ldots (1)$$

where $\varepsilon = \frac{1}{2} m(\xi^2 + \eta^2 + \zeta^2)$,

$$\mu = \frac{h^2}{2m} \left(\frac{3n}{8\pi}\right)^{\frac{2}{3}}$$

k is Boltzmann constant, and n is number of electrons per unit volume. At zero degrees Absolute, equation (1) becomes

$$N(\xi,\eta,\zeta)d\xi d\eta d\zeta = \frac{2m^3}{h^3} d\xi\, d\eta\, d\zeta \quad \text{for } \varepsilon < \mu_o$$
$$= 0 \quad \text{for } \varepsilon > \mu_o \qquad \ldots\ldots\ldots (2)$$

Thus at absolute zero the density of electron distribution in velocity space is uniform with a sphere of radius $\sqrt{\frac{2\mu_o}{m}}$

The number of electrons having energy in the range ε to $\varepsilon + d\varepsilon$ is given by

$$N(\varepsilon)d\varepsilon = \frac{8\pi\sqrt{2}}{h^3}\, m^{\frac{3}{2}}\, \frac{\varepsilon^{\frac{1}{2}}}{e^{\varepsilon-\mu/kT}+1}\, d\varepsilon \qquad \ldots\ldots (3)$$

at temperature T, and

$$N(\varepsilon)\, d\varepsilon = \frac{8\pi\sqrt{2}}{h^3}\, m^{\frac{3}{2}}\, \varepsilon^{\frac{1}{2}}\, d\varepsilon \qquad \ldots\ldots\ldots (4)$$

at absolute zero. The functions (1) and (2) are plotted in Fig. 4.1 and the electron energies in an idealized metal at $0^{o}K$ are shown in Fig. 4.2-a. There are no electrons above $W_e = \mu_o$. The barrier height is W_a, approximately 2 to 6 volts energy higher than μ_o . According to non-quantum mechanical treatment, electrons can escape the metal only by obtaining enough energy to rise to the top of the barrier. For instance when light of energy $h\nu$ is incident upon the metal, electrons will be excited, and some of them will escape from all energy levels higher than $W = \mu_o - d = \mu_o + h\nu - W_o$. (see fig. 4.2-b) By applying a retarding potential Ve, one can expect only those electrons to reach the anode which have energy higher than $h\nu + \mu_o - W_a - Ve$, and thus it should be possible to study the distribution of energy of photoelectrons.

In the interaction of photons with the electrons of a metal, simultaneous conservation of energy and momentum can not be achieved with free electrons. Therefore it is customary, following Tamm and Schubin,[36] to consider two types of photoelectric effects taking place in different force fields. One, the so called volume effect, occurs in the force field of the lattice atoms; the other is the surface photoelectric effect and occurs in the field of the potential barrier. Calculations by Tamm and Schubin indicate that the volume photoelectric effect is of negligible importance in the range of usual photoelectric experiments. Furthermore, no adequate theoretical treatment of the volume effect is available. Theoretical discussion here will be restricted to the surface photoelectric effect.

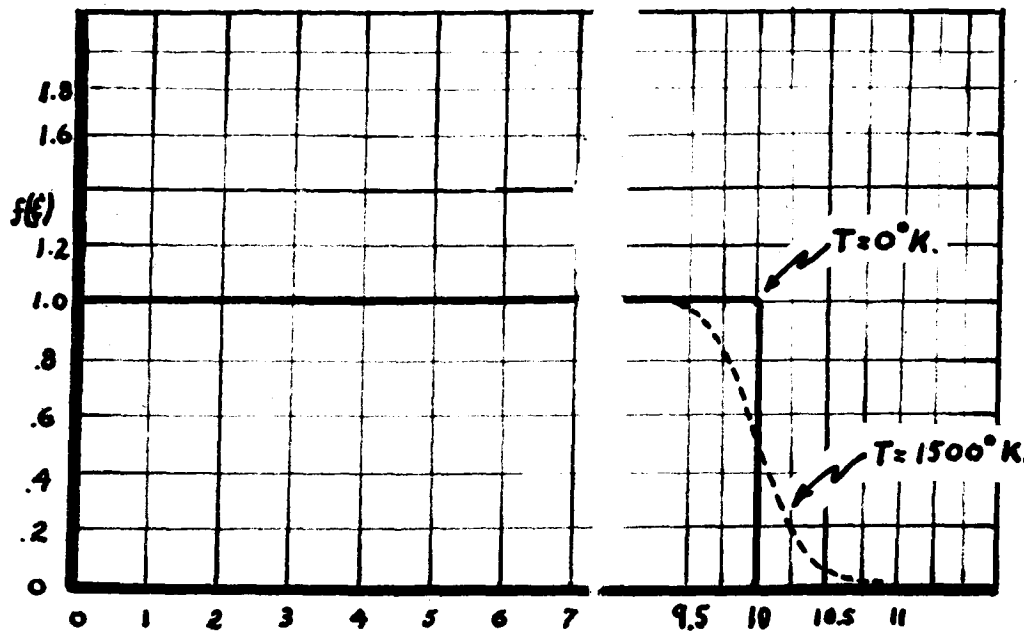

FIG. 4.1 FERMI-DIRAC DISTRIBUTION OF VELOCITY COMPONENTS FOR T=0°K, AND FOR T=1500°K.

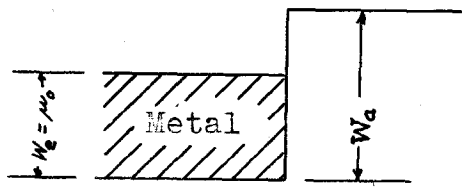

Fig. 4.2 a

Electron energies in an ideal metal at 0°K

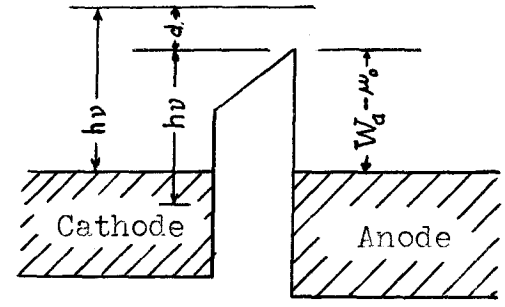

Fig. 4.2 b

Electron energies in photoelectric emission (applied potential equal to contact potential difference)

The following exerpt from the article by Overhage[1] states very nicely the assumptions of the Fowler-Dubridge theory:

"(1) The energy $h\nu$ of the photon is communicated to the electron in such a way that only its momentum normal to the surface is changed.

"(2) The probability that an electron will be put into a state of higher energy by an incident quantum is proportional to the electron's initial velocity normal to the surface.

"(3) The transmission coefficients at the boundary are

$$D(\varepsilon_n, \nu) = 0 \qquad \text{when } (\varepsilon_n + h\nu) < W_a$$

$$D(\varepsilon_n, \nu) = 1 \qquad \text{when } (\varepsilon_n + h\nu) \geq W_a \text{ ."}$$

From the first assumption one will infer that the normal energy of a photoelectrically emitted electron of initial energy ε_n is $\varepsilon_n + h\nu - W_a$; this has been supported by quantum mechanical derivation for the ideal case of plane metal surfaces.

The second assumption has also been shown valid quantum mechanically, although its introduction into the present theory was largely for ease of integration.

Under the above conditions Dubridge obtains the following expression for the current:

$$I = \alpha A T^2 \varphi(\lambda) \qquad \ldots\ldots\ldots \quad (5)$$

where α is the proportionality constant of assumption, (2)

$$A = \frac{4\pi mek^2}{h^3} \qquad \ldots\ldots\ldots \quad (6)$$

the constant of Richardson's equation, and $\varphi(\lambda)$ is Fowler's universal function,

$$e^x - \frac{e^{2x}}{2^2} + \frac{e^{3x}}{3^2} + \ldots\ldots x \leq 0$$

$$\frac{x^2}{2} + \frac{\pi^2}{6} - \left[e^{-x} - \frac{e^{-2x}}{3^2} + \ldots\right] x \geq 0$$

of the argument

$$x = \frac{h\nu + \mu_o - W_a - Ve}{kT}$$

In case $T = 0^oK$ this reduces to

$$I_o = 0 \qquad \text{for } h\nu \leq (W_a + Ve - \mu_o)$$

$$I_o = 2\pi me\alpha\,[h\nu - Ve - W_a + \mu_o]^2 \qquad \text{for } h\nu \geq (W_a + Ve - \mu_o) \quad \ldots \quad (7)$$

V. "NORMAL" ENERGY DISTRIBUTION FROM ROUGH SURFACES

As will be fully discussed in a later section (VI-4) the sodium surfaces used by Overhage in his experiments and by the writer in the present experiments consisted of a visible deposit of white matte appearance evaporated from very pure sodium unto a nickel cathode. The largest of the globules in the matte surface were a fraction of a millimeter in diameter, and hence constituted quite a departure from the ideally plane surface postulated in all previous theoretical treatments of the photo-electric effect.

In order to determine the effect of a rough surface on the normal energy distribution of photoelectrons the following would be ideal procedure:

Let there be a surface element of the cathode inclined to the anode, though the gross anode and cathode surfaces are parallel. Draw a plane perpendicular to this element and to the anode. Let the x-axis be in this plane and perpendicular to the cathode; and the y-axis lie in this plane and along the surface of the cathode element. Call the perpendicular to the anode the normal direction; and call the angle between the normal and the x-axis, δ

It is desired to calculate the minimum tangential component velocity, v_y, which will serve to give an electron with energy $\frac{1}{2}mv_x^2$ travelling outside the metal the necessary resultant normal velocity to overcome a retarding potential Ve. Two dimensions are all that are required; for the z-axis has no component in the normal direction.

Having found this minimum tangential velocity $v_{y_{min}}$, one would then need to integrate over all Fermi velocities from $v_{y_{min}}$ to ∞, and then over all v_x.

Finally, one would assume some angular distribution of emitting area, including shadows, and after taking into account the angle of the electric vector of the illumination, integrate over the angle zero to $\frac{\pi}{2}$.

This seemed much too ambitious an undertaking, so it was decided to try the calculations for absolute zero. The following quasi-geometrical approach to the problem was suggested by Dr. Houston.

At $0^{o}K$, the density of electron velocity distribution is uniform within a sphere of radius $\sqrt{\frac{2\mu_o}{m}}$ as shown in Fig. 5.1a.

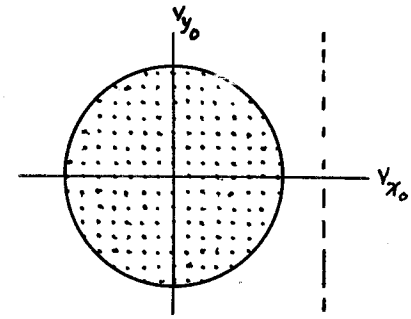

V_o-space
5.1a

Electrons will be excited by incident photons of energy $h\nu$ and will attain increased x- velocities, but will not change their y or z velocities. The excited electrons will lie in a figure like 5.1b. The distribution will no longer be uniform, and the shape of the enclosing system will be distorted.

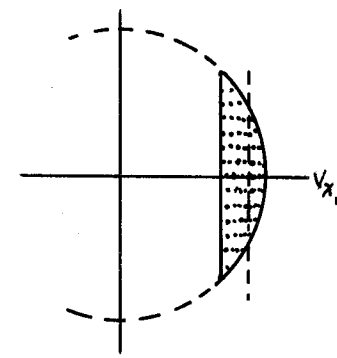

V_1-space
5.1b

The dashed line represents the velocity equivalent to an energy W_a. If there is no retarding potential, electrons to the right of the dashed line can reach the anode. Their velocities will all lie within the Figure 5.1.c. If then a retarding potential $Ve = \frac{1}{2}mv_r^2$ is applied at an angle δ to the x-azis as would be the case for an inclined surface element, only those electrons lying in the hatched portion between the plane, p, and the curved surface can contribute to the photoelectric current.

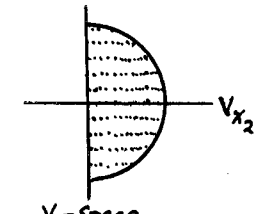

5.1c

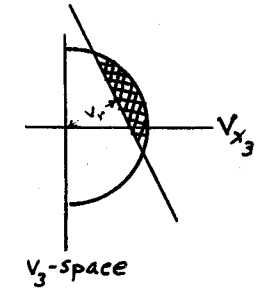

5.1d

It is desired to find the shape which the plane p acquires when we transform v_3 - space back to v_0 - space.

The transformations are:

y - velocity (momentum) is unchanged

z - velocity (momentum) is unchanged.

An electron which in v_0 - space had velocity v_{x_0} given by $\frac{1}{2}mV_{x_0}^2$ has in v_3- space a velocity given by

$$\frac{1}{2}mv_{x_\beta}^2 = \frac{1}{2}mv_{x_0}^2 + h\nu - W_a$$

$$= \frac{1}{2}m\left(v_{x_0}^2 + \frac{2h\nu}{m} - \frac{2W_a}{m}\right) \qquad \ldots\ldots\ldots\ldots (1)$$

So the transformation is

$$v_{x_3} = \left(v_{x_0}^2 + \frac{2hv}{m} - \frac{2W_a}{m}\right)^{\frac{1}{2}} \equiv \left(v_{x_0}^2 - w\right)^{\frac{1}{2}}$$

$$v_{y_3} = v_{y_0}\,, \quad v_{z_3} = v_{z_0}\,, \quad W^2 = \frac{2}{m}\left(W_a - hv\right) \qquad \ldots\ldots\ldots (2)$$

Consider any plane lying perpendicular to the $v_{x_3}\ v_{y_3}$ - plane, distant P from the origin, and making an angle δ with the v_{y_3} axis. The equation of the plane is then

$$v_{x_3}\cos\delta + v_{y_3}\sin\delta = P \qquad \ldots\ldots\ldots (3)$$

Transforming to the unexicited distribution within the metal, the plane will become a cylinder with generators perpendicular to the $v_{x_0}\ v_{y_0}$ - plane.

$$\left(v_{x_0}^2 - w^2\right)\cos\delta + v_{y_0}\sin\delta = P \qquad \ldots\ldots\ldots (4)$$

Drop the zero subscript; and write x, y for v_x, v_y.

$$\left(x^2 - W^2\right)^{\frac{1}{2}}\cos\delta + y\sin\delta = P \qquad \ldots\ldots\ldots (5)$$

We want the volume between this transformed plane and the sphere. Assume the probability of excitation is proportional to v_x with proportionality constant α . (Thanks again to Dr. Houston.)

There will be two cases to consider, depending upon whether the plane in v_3 - space intersects the $v_{y'}$ - axis (i.e. the plane w in fig. 52) outside or inside the sphere, for no electrons can ever escape from the region to the left of w.

Case I. Volume does not touch the plane w in v_o- space w hich is determined by the minimum velocity of "escapable" electrons. (figure 5.2). This is the case of most interest since it applies when surfaces are not too rough and when retarding potentials are not extremely small.

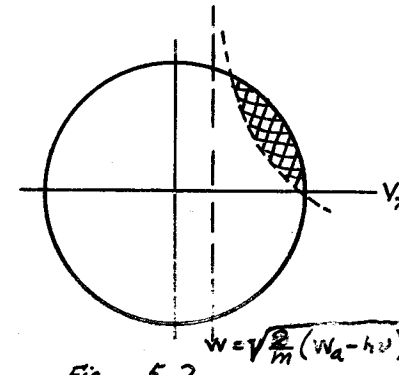

Fig. 5.2

$$I_1 = 2 \int_{y_m}^{y_M} dy \int_{x_m}^{x_M} \alpha x \, dx \int_{o}^{z_M} dz \qquad \ldots\ldots\ldots (6)$$

where

$$z_M = (a^2 - y^2 - x^2)^{\frac{1}{2}} \qquad \ldots\ldots\ldots (7)$$

$$x_M = (a^2 - y^2)^{\frac{1}{2}} \qquad \ldots\ldots\ldots (8)$$

$$x_m^2 = \frac{P^2 - 2Py \sin\delta + y^2 \sin^2\delta + w^2 \cos^2\delta}{\cos^2\delta} \qquad \ldots\ldots\ldots (9)$$

$$y_M = P \sin\delta + \cos\delta \sqrt{a^2 - P^2 - w^2} \qquad \ldots\ldots\ldots (10)$$

$$y_m = P \sin\delta - \cos\delta \sqrt{a^2 - P^2 - w^2} \qquad \ldots\ldots\ldots (11)$$

Hence

$$I_1 = 2\alpha \int_y dy \int_x x \sqrt{a^2 - y^2 - x^2} \, dx \qquad \ldots\ldots\ldots (12)$$

$$I_1 = -\frac{2}{3}\int_y \alpha(a^2 - y^2 - x^2)^{\frac{3}{2}} \Big]_{x_m}^{(a^2-y^2)^{\frac{1}{2}}} dy \qquad x_m = \left[\frac{P^2 - 2Py\sin\delta + y^2\sin^2\delta + w^2\cos^2\delta}{\cos^2\delta}\right]^{\frac{1}{2}}$$

. . . . . (12)

$$= \frac{2}{3}\alpha \int_y \left[a^2 - y^2 - \frac{y^2\sin^2\delta - 2Py\sin\delta + P^2 + w^2\cos^2\delta}{\cos^2\delta}\right]^{\frac{3}{2}} dy \quad . . . . (14)$$

$$= \frac{2\alpha}{3\cos^3\delta} \int_y \left[-y^2 + y(2P\sin\delta) + (w^2\cos^2\delta + a^2\cos^2\delta - P^2)\right]^{\frac{3}{2}} dy \quad . (15)$$

By Pc. 166 and 161 this integrates to:

$$\frac{2\alpha}{3\cos^3\delta}\left\{\frac{y - P\sin\delta}{4}\sqrt{X}\left[-y^2 + y(2P\sin\delta) - P^2 - \left(\frac{3}{2}P^2 + \frac{5}{2}w^2 - \frac{5}{2}a^2\right)\cos^2\delta\right]\right.$$

$$\left. - \frac{3}{2}\left[a^2 - w^2 - P^2\right]^2\cos^4\delta \sin^{-1}\left(\frac{-y + P\sin\delta}{(a^2 - w^2 - P^2)^{\frac{1}{2}}\cos\delta}\right)\right\}_{y_m}^{y_M} \quad . . \quad (16)$$

where X is the terms in [ ] in the integrand

Putting in the limits, only the arc sin term remains, and

$$I_1 = \frac{\alpha\pi}{4}\cos\delta\left[a^2 - W^2 - P^2\right]^2 \qquad . . . . . (17)$$

Now

$$a^2 = \frac{2\mu_o}{m}, \quad w^2 = \frac{2}{m}(W_a - h\nu) \quad ; \quad P^2 = \frac{2}{m}Ve \qquad \ldots\ldots\ldots (18)$$

α = angle between anode and cathode elements

V = retarding voltage.

Therefore

$$I_1 = \frac{\alpha\pi}{4}\cos\delta\,[\mu_o + h\nu - W_a - Ve]^2 \frac{4}{m^2} \qquad \ldots\ldots\ldots (19)$$

$$= \frac{\pi\alpha}{m^2}\cos\delta[\mu_o + h\nu - W_a - Ve]^2 \qquad \ldots\ldots\ldots (20)$$

and the current becomes

$$i = \frac{3ne\alpha\cos\delta}{4\pi a^2 m^2}\cos\delta[\mu_o + h\nu - W_a - Ve]^2 \qquad \ldots\ldots\ldots (21)$$

$$= \frac{3ne\alpha\cos\delta}{4(2m\mu_o)^{\frac{3}{2}}}[\mu_o + h\nu - W_a - Ve]^2 \qquad \ldots\ldots\ldots (22)$$

$$= \frac{2\pi em\alpha}{h^3}\cos\delta[\mu_o + h\nu - W_a - Ve]^2 \qquad \ldots\ldots\ldots (23)$$

This is just the expression (4.7) which Dubridge obtains, multiplied by a factor cos δ

The photoelectric current from a rough surface at 0°K thus shows the same dependence on retarding potential and on incident energy as that from a smooth surface, for not too rough surfaces, and not too ~~well~~ small retarding potentials (i.e. in the nigh energy region).

Case 2. The volume has the plane, w as one boundary.

We will treat this case by subtracting from I, the part, I_2 lying behind the plane w.

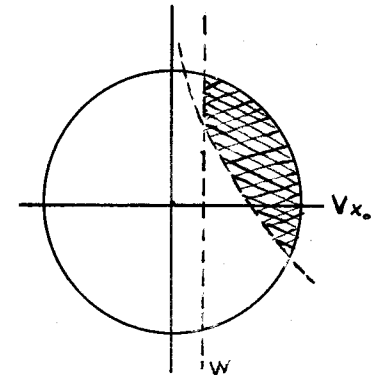

$$I_2 = 2 \int_{y'_m}^{y_M} dy \int_{x_m}^{x'_M} \alpha x dx \int_0^{z_M} dz \quad . . (24)$$

where z_M, x_m and y_M are given as before by (7), (9), (10). The new upper limit on x is

$$z'_M = W \; ; \quad . . . . . (8a)$$

and y_m is given by the intersection of W and the transformed plane.

$$y'_m = P/\sin\delta \quad . . . . . (11a)$$

The results of the integration are not simple; hence they will be merely indicated here.

One obtains

$$\frac{I_1}{2} + \frac{2a\cos\delta}{4}\left\{\frac{P}{4\sin\delta}\sqrt{X}\left(\frac{-P^2}{\sin^2\delta} - \frac{3}{2}P^2 - \frac{5}{2}W^2 + \frac{5}{2}a^2\right)\right.$$

$$\left. - \frac{3}{8}(a^2-W^2-P^2)\sin^{-1}\left(\frac{-P\cot\delta}{(a^2-W^2-P^2)^{\frac{1}{2}}}\right)\right. \qquad \ldots\ldots\ldots\ldots (25)$$

$$\left. \pm \frac{a}{12}\left[2y(a^2-W^2-y^2)^{\frac{3}{2}} + 3(a^2-W^2)(a^2-W^2-y^2)^{\frac{1}{2}}y + 3(a^2-W^2)^2\sin^{-1}\frac{y}{a^2-W^2}\right]\right\}_{y'_m}^{y_M}$$

where

$$\sqrt{X} = \cos\delta\left(a^2-W^2 - \frac{P^2}{\sin^2\delta}\right)^{\frac{1}{2}}$$

$$y'_m = P/\sin\delta$$

and

$$y_M = P\sin\delta + \cos\delta\sqrt{a^2-P^2-w^2}$$

The last term of (25) does not become simpler upon putting in the limits.

When the transformed plane lies entirely behind w, we have the condition of no retarding field at all. As the transformed plane recedes still farther, we have the case of accelerating fields; and we can conclude from our analysis that at least for small fields the current is independent of the field. This is as it should be.

Let us investigate quantitatively under what circumstances Case 1 holds: it will be valid whenever the transformed plane strikes the circle

below where w does, i.e., whenever

$$P/\sin\delta \geq P\sin\delta + \cos\delta \sqrt{a^2-P^2-w^2} \quad \ldots\ldots (26)$$

Multiplying by sin δ , transposing and putting

then squaring, we get

$$P^2\cos^2\delta \geq \sin^2\delta \cos^2\delta (a^2-P^2-w^2) \quad \ldots\ldots (27)$$

Canceling $\cos^2 \delta$, transposing $P^2 \sin^2\delta$, and calling $\sin^2\delta + \cos^2\delta = 1$

we have

$$P^2 \geq (a^2-w^2) \sin^2\delta \quad \ldots\ldots (28)$$

Putting in the values of P, a, and w from (18) we have finally that Case 1 is valid whenever

$$Ve \geq \sin^2\delta (\mu_o+h\nu-W_a) \quad \ldots\ldots (29)$$

i.e,

$$Ve \geq \sin^2\delta (h\nu-h\nu_o) \quad \ldots\ldots (30)$$

where ν_o is the threshold frequency. The threshold of the sodium used in Overhage's data* is approximately 6700 A^o. This represents a work function of 1.83 volts, which compares favorably with the value 1.8 volts given by Millikan[47].

For a surface whose irregularities are as high as 45^o, the minimum retarding voltage is $\frac{1}{2}(h\nu - 1.83)$. For the λ_{5461} this is

---

* The author expresses his thanks to J.E. Thomas for calculating this threshold.

0.2 volt, so that all but perhaps the highest two points fall under Case 1. Corresponding points on the normal emission curves for shorter wave lengths than 5461 A^{o} were obtained by applying increased retarding potentials of magnitude given by the difference in energy of the λ_{5461} and the shorter λ's. That is

$$\Delta Ve = (h\nu - h\nu_{5461})$$

Hence any point which is valid on the λ_{5461} curve will be valid for shorter wave-length curves.

Deviations from Case 1 will be in the form of decrease in emitted current, photoelectric saturation curves for rough surfaces will be rounded even at $0^{o}K$. The top two points of Overhage's published data are below corresponding points of higher frequency curves; but it is questionable whether this is attributable to failure of Case 1 or to approaching saturation.

VI. THE EXPERIMENTAL ARRANGEMENT

Several years before the present experiments, images of cathodes were obtained by thermionic and cold emission as well as from photoelectric emitting surfaces. Thermionic cathodes expecially have been extensively investigated. (Myers[27] gives more than 40 references to experiments between the years 1933 and 1940.) Some of these experiments are briefly described in 3.11, and are of no interest here other than to recall that they indicate crystal structure of emitting surfaces due to differences in work function over the surface. The design is essentially different in photoelectric emission, due to the necessary space for illumination; and considerable less work has been done with this apparatus. Since emission varies as the normal component of the electric vector, the mmost efficient angle for illumination should be glancing incidence; however, the intensity of the illumination falls off at low angles so that the most efficient angle of illumination is approximately 3.5° from tangential. Room must be left for a quartz window and a condensing lens so the angle is usually made smaller. Hence it is not feasible to superimpose the electrostatic accelerating field and the field of the magnetic lens, nor is it feasible to use an electrostatic immersion lens. Furthermore, photoelectric emission current is at best exceedingly small so that in order to get sufficiently intense fluorescent images, fairly high potentials must be used.

The first photoelectric cathode images seem to have been obtained by Brüche [48] in 1933 when he took fair quality pictures of a perforated zinc plate. Pohl[49-50] in 1934 obtained quite good images of the emission from aluminum, copper and zinc surfaces. He drew very few

conclusions, noting merely that the illumination was highly dependent upon the purity of the surface and that such small contaminations as the grease and acid from finger prints were sufficient to decrease the emission from the touched portion. Pictures 6.1, e, f, and g. taken in this laboratory during the course of some preliminary experiments indicate this effect quite clearly.

In 1935 Mahl and Pohl[51] conducted some investigations on the photoelectric emission from various minerals and noted that the structure was quite clearly shown. Except for this last experiment, all electron optical investigations of photoelectric emission seem to have been purely to demonstrate the possibility of imaging photoelectric surfaces.

6.1. Preliminary Experiments.

In this laboratory the first apparatus which was designed for the study of photoelectric surfaces was much like that of Pohl. It was a glass tube 1 3/4" in diameter and 20" long. The inside of the tube was painted with aquadag which served as a ground and/a light shield. One end of the tube held the anode. The anode shape was roughly parabolic, as designed by Gray[28] for reduced aberration. A flat perforated anode was also tried briefly but was discarded. A large (4 mm diameter) anode hole was used to get high electron current .

Both flat and convex cathodes were tried and found equally good; they consisted of brass surfaces with small hole which could contain either

a hot filament or a zinc plug. Cathode-anode distance was approximately 2 centimeters. The whole cathode end could be removed by means of a ground glass joint which ordinarily was sealed with black wax. A side tube inclined at approximately 15 degrees to the cathode surface had waxed on its end a quartz window to allow illumination of the emitting surface. The system was evacuated by means of a two-stage mercury vapor pump and a "Hy Vac" rotary oil pump.

The voltage supply was 10 KV from a voltage doubler circuit which had been constructed for previous experiments. Focussing was accomplished by means of a shielded iron lens (see Figure 6.1a) of essentially the type which was first described by Knoll and Ruska[52]. Its pole piece diameter was just sufficient to fit outside the glass. Pole spacing was approximately 5 mm. This same magnetic lens has been used in all subsequent experiments.

Images were viewed from the back side of a fluorescent screen which closed the far end of the tube. The technique of forming fluorescent screens will be discussed later. Images, although not very satisfactory ones, were obtained from the hot filament. A cold mercury vapor discharge tube (approximately 85% of illumination is in 2536 A^{o} mercury line) showed some photoelectric emission from the zinc surface. However, emission was so low in intensity that it could not be visually focused and certainly could not be photographed.

This apparatus demonstrated that some means must be found to eliminate light which scattered from the cathode and struck the fluorescent screen. It also showed that the photoelectric intensity from the zinc surface was not sufficient with 10 KV exciting potential and the existing

illumination to enable one to focus by means of photoelectric emission. Hence in the next model the entire glass tube from anode to viewing screen was curved with a radius of approximately 5 meters and was fitted with several nickel apertures. The tube was oriented in a north-south direction so that the earth's field would bend the electron beam somewhat in the curvature of the tube, and auxiliary deflecting coils were wound around the tube for further bending the beam and for raising and lowering the image.

An electron beam will be curved horizontally without distortion by a uniform vertical magnetic field. The required current density along a cylinder, in order to produce a uniform magnetic field inside can be easily calculated, (See section 7) and is given by

where $i_z(\theta)$ is the current density down one side and back the other along the cylinder, expressed as a function of θ, the angle made by the radius vector to the current element. B is the desired field.

Wires were laid along the tube to approximate the current distribution of (1); and served to bend the beam quite satisfactorily, the only objection being the difficulty of removing them and replacing them when the apparatus was baked out. The author recently discovered that Mahl and Pohl[51] had also found it necessary to curve their electron beam to eliminate stray light. They accomplished it by bending the beam sharply through approximately 30° with a Helmholtz coil near the image end of the tube.

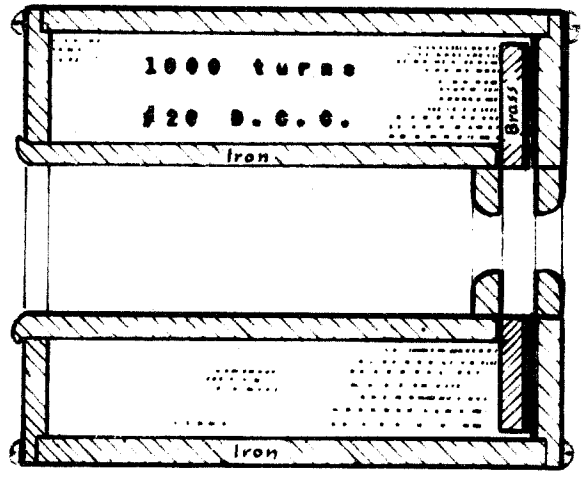

Fig. 6.1a. Magnetic objective lens.

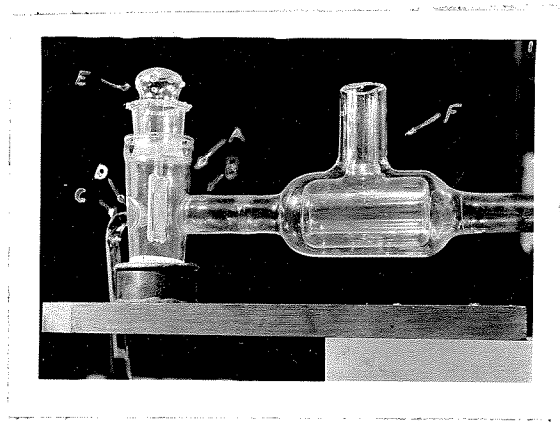

Fig. 6.1 b Camera and Trap

Provision was made for inserting the cold mercury arc directly into the vacuum a few centimeters from the cathode; and the cathode was made so that either the zinc surface or the hot filament could be swung into position for imaging .

Fairly satisfactory images were obtained but screen fluorencense was still so low that the time required for photographic exposures was an hour or more. It appeared undesirable to try to maintain power supply voltage, magnet current and deflecting coil currents constant over so long a period, so a camera was built whereby photographic plates could be directly exposed to the electron beam.

To Mr. Clancy is due great thanks for construction of the camera and liquid air trap which were used. The camera consisted, as shown in Figure 6.1b,of a couble stop cock. The outer wall of the outer stop cock A had 2 side tubes B, C, the first of which was sealed on to the apparatus and the second at an angle of 120° to B led to an auxiliary vacuum pump. The inner wall of the outer stop cock had a hole,D, which could be turned to either side tube, thus allowing the electron beam to enter the camera, or shutting the camera off from the vacuum system and opening it to the auxiliary pumping system. In this latter position, air could be let into the camera and the inner stop cock E removed in order to change photographic plates. The inner stop cock could be turned to expose either a fluorescent screen or a photographic plate to the electron beam. The liquid air flask F was made so that it allowed free passage of the electron beam. The liquid air was contained in a do-nut shaped flask suspended by its neck from the top. The vacuum system of the apparatus itself served as thermal insulation.

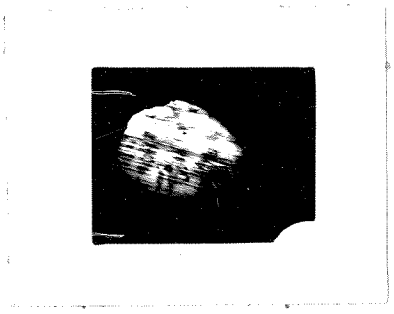

c

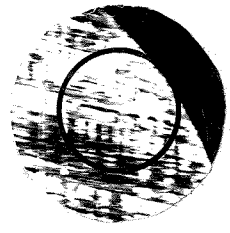

d

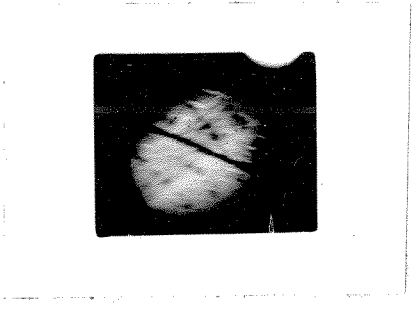

e

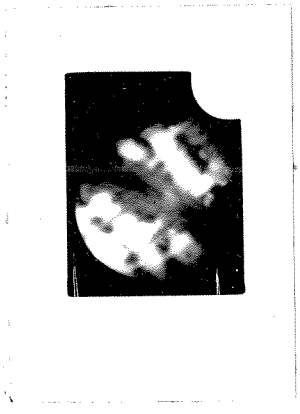

f

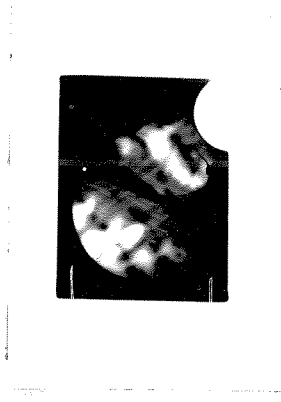

g

Fig. 6.1 c, d, e, f, g

With this apparatus, good images were obtained of the emission from zinc surfaces, with 5 to 20 seconds exposure. It was found that freshly scraped zinc gave an image much like that seen optically by illuminating at the same angle. Brüche[37] had noted this fact. Figure 6.1c is the electron image at 10 diameters magnification of a portion of a zinc surface which had been freshly scraped with a knife before inserting it in the vacuum. After the electron picture was taken, the zinc was removed and the same portion photographed optically. Figure 6.1d is this optical picture magnified approximately 10 diameters. The approximate portion which was photoelectricaly imaged is ringed with ink in the optical picture. Unfortunately neither the portion nor the illuminating angle was exactly the same for electron and optical pictures, so that a similarity of form of emission is all that can be noted.

It was found that minute grease contaminations optically undetected were sufficient to almost completely stop electron emission. Other investigators have noted this fact. Figures 6.1e,f,g. illustrate the spreading of a thin grease streamer and the etching of human finger prints upon zinc. The first picture was taken immediately after putting the prepared zinc surface in the microscope. In the second picture taken 1/2 hour later, it will be noticed how the grease has spread out over the cathode and run down the minute scratches left by the cleaning knife. It can also be seen that the finger print has etched in more deeply. In the third picture taken 1/2 hour later with the vapor pumps off in the interim, the process has continued still further, the grease streamer spreading out more and running down the scratch markes to a greater extent.

The original grease streamer was visible when it was put on the zinc surface but the spreading was not visually apparent after the zinc was removed from the microscope, nor could the finger print be seen.

One run was made, heating a zinc surface overnight by means of a Tungsten filament in order to see whether changes in image pattern were were detectable. Unfortunately, the vacuum fell off very badly during the run. It was thought that some changes in the electron image were visible, but no pictures were taken. Finally, the vacuum was repaired, the zinc surface cleaned, a sodium ampoule made following Overhage's technique, and some sodium was distilled on the zinc.

Only one photograph was obtained with this sodium zinc surface. Sodium spread so badly over the walls of the apparatus that leakage from cathode to ground occurred. The original cathode end of Overhage's tube was available and had been designed for very high leakage resistance so it was installed.

In working with sodium, the fact that a vacuum of the quality desired could not be maintained with the stop cock camera became apparent, so although it made a difference of a factor of at least 50 in exposure time, the camera was removed and a permanent fluorescent screen inserted. This time, however, the screen was viewed from the front, thereby increasing efficiency by a factor of about 4. Voltage supply was increased to 40 KV; and with this arrangement, images were obtained from sodium surfaces in as little as 2 seconds.

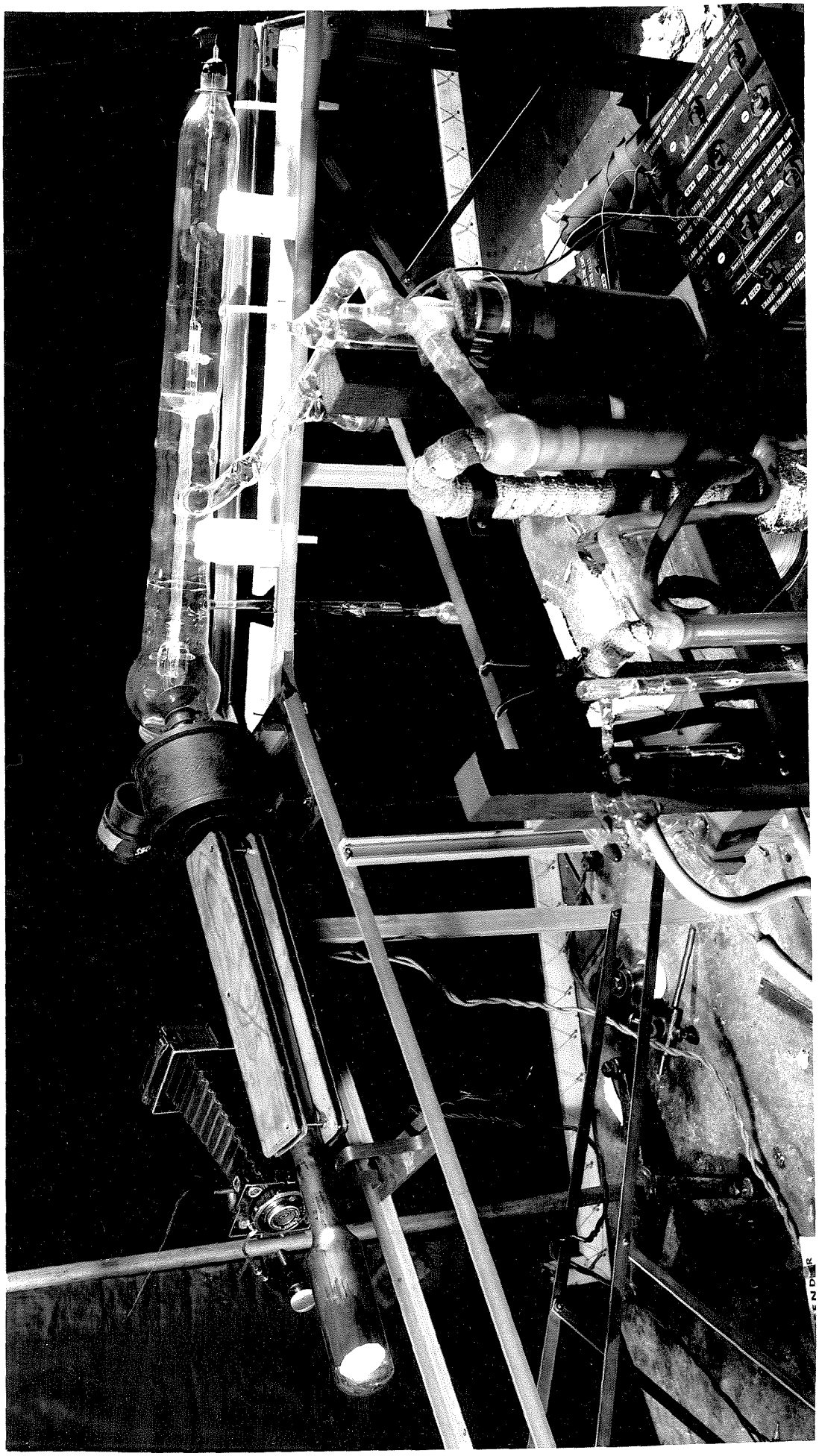

Fig. 6.2 a

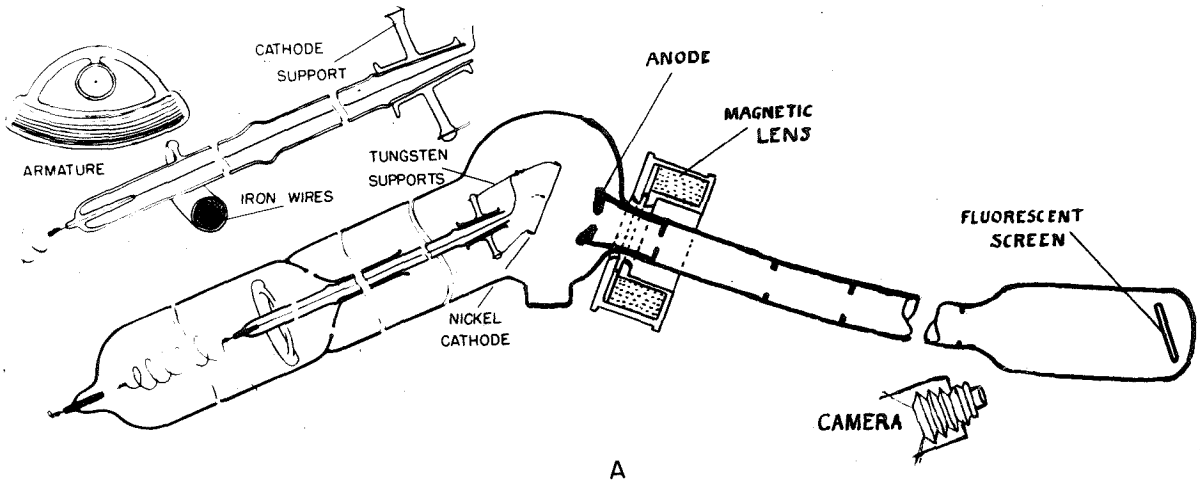
CATHODE
SUPPORT
ARMATURE
IRON WIRES
TUNGSTEN
SUPPORTS
ANODE
MAGNETIC
LENS
FLUORESCENT
SCREEN
NICKEL
CATHODE
CAMERA
A

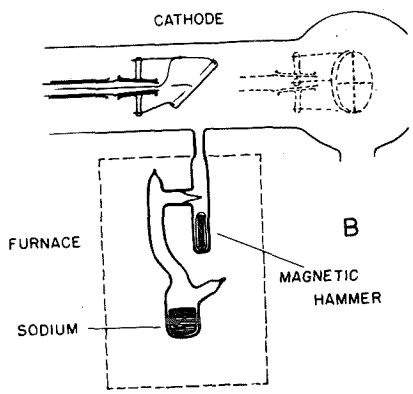
CATHODE
FURNACE
B
MAGNETIC
HAMMER
SODIUM

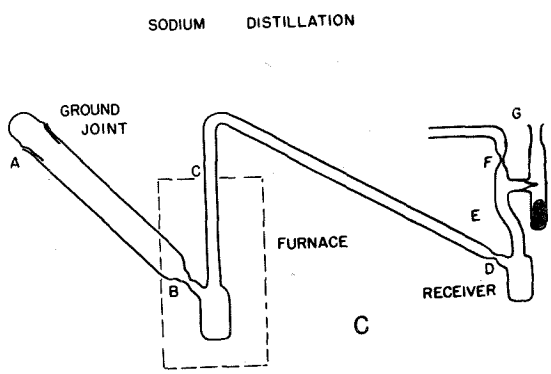
SODIUM DISTILLATION
GROUND
JOINT
A
C
G
F
E
FURNACE
D
B
RECEIVER
C

Fig. 6.2 b

6.2. Final Form of the Apparatus.

The final apparatus is shown in Figure 6.2a and in some detail in Figure 6.2b. The long large tube is Overhage's cathode assembly, designed to furnish well insulated path from cathode to anode and ground. The cathode plate itself was a disk, made in four quadrants from nickel sheet. This form of cathode was the last one used by Overhage; it was so designed that it would do a minimum amount of buckling upon heating with an induction furnace for outgassing. For the purposes of cathode imaging it was not extremely satisfactory, since the lack of smoothness distorted the image. It will be noted that all pictures of sodium here presented are images of one quadrant, the other three quadrants being out of the field of view. It was found necessary to spin the edges of the cathode in order to avoid cold emission to the walls of the apparatus. Even after spinning, some cold emission was noticed; it built up charges on the glass which made the image position unstable. The trouble was traced to a fine wire being used to fasten part of the cathode mount. Rather than take the apparatus apart, the glass tube in the vicinity of the wire was painted with aquadag, and connected to the cathode potential. This worked very satisfactorily.

By means of an external electromagnet the cathode could be pulled back into position to apply sodium, (see Section 6.4) or up into operating position approximately parallel to the anode and 3/4" from it. The inability to maintain the cathode accurately centered and parallel to the anode, or to return it twice to exactly the same

position, was one of the most serious objections to this model of the apparatus.

The anode is shown in Figure 6.2b. It was made of monel turned quite thin, and carried an apertured supporting tube which made spring fit inside the glass tube. The inside of the tube was silvered except for the part near the flourescent screen, to furnish good ground contact throughout, and was fitted with several 1/2" apertures made of nickel sheet. The apertures were held in place by #10 nickel wire wound in the form of helices which made spring fit on the tube. Apertures and helices served as traps to keep any light at the cathode from reaching the flourescent screen. The glass near the flourescent screen was painted very lightly with aquadag. The helix nearest the anode carried a wire which was silver soldered on to the anode, and borught out through the glass to the ground. It was found essential to maintain a very good ground connection.

The fluorescent screen was set with its normal at an angle of about 10° to the electron beam, and was contained in a tube about $2\frac{1}{2}$" in diameter, for photographing with an external camera. The large tube was quite free from flaws, and could be satisfactorily photographed through.

All apertures were spotted with fluorescent powder to facilitate locating the image; they could be seen through scratches in the silvering. The angle of the flourescent screen no doubt contributed to the fact that images were not in uniform focus over their entire areas; but since the camera had to be used wide open

to obtain sufficient speed, it was considered wise to incline the screen so that it was nearly perpendicular to the camera rather than to the beam. The depth of focus of the electron image was considerably more than that of the camera.

The window for illuminating the cathode proved quite a serious problem. For two reasons -- it was undesirable to use a pyrex graded seal. First, it was advantageous to use the quartz condensing lens as close to the cathode as possible outside the vacuum. Second, no graded seal was at hand, and seals are expensive. Quartz windows sealed to pyrex with silver chloride were tried because silver chloride, melting at 450°C., could stand the temperature necessary in baking out the glass. However, the glass cracked. Calculations on the strength of quartz indicated that quartz bubbles blown very thin could be sealed directly into pyrex tubes. Some bubbles were made and it seemed probable that this would be satisfactory. This idea was discarded, however, because of the danger to the apparatus in case a bubble broke. Finally a special glass window which transmitted more than 10% of the 2536 A° line and could be sealed directly to pyrex was obtained from Corning Glass Works and proved very satisfactory.

The vacuum in the system was maintained by two mercury diffusion pumps backed by a Hyvac rotary oil pump. Two liquid air traps were inserted between the vapor pumps and the apparatus, and the vacuum was measured with an ionization gauge. After two days baking out at 400°C, and heating the cathode with an induction furnace, sodium was distilled into the apparatus. Pictures were taken under conditons when the vacuum

was better than 10^{-6}mm.; over a period of a week the images showed no decrease in intensity. Three runs were made. In order to have an accurate check on intensity of images, and in order to have all photographic negatives as nearly as possible of the same density, an exposure meter was made consisting of a pair of polaroid plates, behind which was fixed a cold mercury arc flourescing a piece of Willemite for standard light. One polaroid plate was rotated until the electron image and the standard light seemed to be of the same intensity. The angle of rotation was then a measure of intensity of the electron image.

6.3. The power Supply.

The power supply used in these experiments was one which had been built up for the large electron microscope. It consisted of a cascade voltage doubler circuit in two sections, the upper section floating always at 20 KV above ground. The voltage doubler circuit was of standard variety using two kenetrons, and having the positive side grounded. Freedom from ripple was obtained merely by use of very large condensers, and drawing very small loads. Thus far, no voltage regulator has been used with the power supply. The output voltage was hence approximately 40 KV, but varied by at least the same percentage as the 110 V. primary power supply. In operation approximately 100 meg ohm resister was used in series with the power supply to avoid breaking down from any possible

gas discharges in the apparatus.

6.4. Preparation of Sodium.

The sodium used was prepared from a commercial product, after the method devised by Overhage, in a separate pyrex distillation apparatus shown in Figure 6.2b. The sodium, normally kept under kerosene, was washed in dry petroleum ether and then pared free of oxide. It was then put into the test tube A, (Figure 6.2b.) which was immediately closed by a cap and pumped by a good vacuum system. After the whole system was evacuated the metal was fused in the bottom of the tube just above B, by means of a Bunsen flame. Most of the impurities remained behind in the test tube while the sodium ran down. The test tube was then pulled off at B by means of an oxygen flame. An electric furnace was placed around the sodium bulb and the metal heated to 400°C. for about six hours, the vapor condensing in the section between the top of the furnace c, and the bend in the tube. At the end of six hours, most of the hydrogen and hydro-carbon vapors had been pumped out, whereupon the metal was distilled into the receiver by a heater wire around the condenser tube. When a sufficient supply of sodium had been accumulated in the receiver, the still was sealed off at D, and removed from the pumps at F. The sodium supply was then in an evacuated container ready to be attached to the photoelectric apparatus.

When it was desired to deposit sodium upon the cathode, the breakable tip of the sodium container was cracked off with a glass-covered magnetic hammer and the furnace was put around the sodium container as shown in the figure. A visible deposit of matte white appearance formed upon the cathode during two hours heating with the furnace. The cathode was moved back and forth occassionally to enable the sodium to cover all parts of the surface.

6. 5. Source of Illumination.

Illumination was obtained both from hot and from cold quartz mercury arcs focused by means of a quartz lens upon the cathode. The cold mercury arc was supposed to radiate more than 85% of its energy in the 2536 A° line, and gave no visible image intensity when filtered by Eastman 18A (3650 A°) filter or Vitaglass (transmitting down to below 3000 Å) The hot mercury arc produced about 20 times as intense photoelectric current from sodium as did the cold arc, and had considerable intensity from 2536 A° through visible wave lengths.

The filters used were

18A -- transmits little except the 3650 A° line

50 -- transmits little except 4050 A° and 4360 A° blue lines

77 -- transmits only 5460 A° line, green

Vitaglass -- transmits below 3000 A° (45% of 3000 A°, and none of 2536)

Windowglass -- transmits down to 3100 A° (transmits approximately 30% of 3300, none below 3100).

6.6. Fluorescent Screens.

Considerable work has been done both on the theory and practical problems concerned with flourescent screen making by workers in television.* The problem here was the same as in much television work, namely that of producing a fine-grained screen which would have high photographic intensity. In the preliminary experiments, it was also desirable to have the screen thin and homogeneous so that it could be viewed from the rear. Zinc sulphide and synthetic Willimite (zinc orthosilicate) obtained from the electrical engineering department were laid down approximately to the directions given by Leverenz[53] using a very fine suspension of the material in a beaker of distilled water. After 12 hours, most of the phosphor had settled on the bottom of the beaker and the water was decanted off by allowing it to run slowly through a capillary tube in the bottom of the beaker. It was not found necessary to use anything more pure than ordinary distilled water. The only difficulty with this method was in obtaining a sufficiently fine suspension of the phosphor; it was ground in a quartz mortar and the suspension was allowed to stand for about 10 minutes to settle the heavy parts before pouring it over the blank. In preparing screens for front viewing, no care was required to see that the proper thickness was achieved, so a fair amount of powder was mixed with distilled water. After drying, screens so made would stand washing with a gentle stream of water without harm.

---

* See e.g. V.K. Zworykin and G.A. Morton, Television, Wiley & sons 1940

6.7. Coil for Deflecting Electron Beam.

The problem here was to find the form of current $i_z(\theta)$ for a deflecting coil to fit around the tube and to supplement the earth's field, i.e. to give uniform vertical field inside the tube. The current was to go down one side of the tube and back the other. By Smythe (loc cit. Article 7.10) we can form the general expression for the vector potential A_z due to current distribution along an infinite circular shell of radius a.

$$i_z = \Sigma\, c_n \cos n\alpha \qquad \ldots\ldots\ldots (1)$$

$$A_z = 4\pi a\, C_o \ln a + 2\pi a \sum_1^\infty \frac{1}{n} \left(\frac{r}{a}\right)^n C_n \cos n\theta \qquad \ldots\ldots\ldots (2)$$

It is desired here that

$$B = B_r \sin\theta - B_\theta \cos\theta \qquad \ldots\ldots\ldots (3)$$

where B can be written as the curl of **A** from 3.5 (4) of this thesis.

$$B_r = \frac{1}{r}\frac{\partial A_z}{\partial \theta} = \frac{2\pi a}{r} \Sigma\, c_n \sin n\theta \left(\frac{r}{a}\right)^n \qquad \ldots\ldots\ldots (4)$$

$$B_\theta = -\frac{\partial A_z}{\partial r} = -\frac{2\pi a}{r} \Sigma\, c_n \cos n\theta \left(\frac{r}{a}\right)^n \qquad \ldots\ldots\ldots (5)$$

We want n equal to 1 in order that the current will go down one side and back the other; then from (4), (5), and (3),

$$B_r = -2\pi c_1 \sin\theta \qquad \ldots\ldots\ldots\ldots (6)$$

$$B_\theta = -2\pi c_1 \cos\theta \qquad \ldots\ldots\ldots\ldots (7)$$

$$c_1 = B/2\pi \qquad \ldots\ldots\ldots\ldots (8)$$

Therefore

$$i_z = \frac{B}{2\pi}\cos\theta \qquad \ldots\ldots\ldots\ldots (9)$$

This is the desired current distribution, where B is the required field and θ is the angle in cylindrical coordinates. It was approximated experimentally by laying wires along the tube spaced according to a cosine distribution. A single strand of wire was used by stretching it down one side of the tube, wrapping it around, and bringing it back the other; then around and down again, and so on. Vertical deflection for centering the image was accomplished by a similar coil rotated through 90°. The writer used eight turns of wire and found that the beam was quite uniformly deflected.

As mentioned earlier in this work, there was difficulty in removing and replacing these coils when the apparatus was baked out; hence, in the final apparatus, a new design was tried consisting of two flat coils of 75 turns each wound on wood forms 2 1/2" wide and 12" long, and laid above and below the tube. Vertical deflection was accomplished merely by twisting the two coils slightly out of horizontal position. This deflecting mechanism was satisfactory.

VII. RESULTS

Plates 7.1 and 7.2 are photoelectric pictures of a sodium deposit on nickel under different frequencies of illumination from 2536 A^{o}, to 4078 A^{o}, and at different ages from seven hours through 80 hours. Pictures were taken during this run at less than 7 hours, but exposure times and focusing current had not yet been standardized and were sufficiently different from the above that a comparison could not be made. The magnification was 10 ± 2 diameters electron optically, photographically enlarged 2 times, giving a total magnification of 20 diameters. Photographic exposures were adjusted between the limits of 2 and 20 seconds, at f4.5 with superpan press film, so that negatives all had approximately the same density; and developing times were carefully controlled. The plates 7.1 and 7.2 are one quadrant of the cathode, illumination coming from the upper right hand corner of the photograph. All show matte emission, and the image is much like that due to illumination by light at a low angle; the importance of theoretical treatment of photoelectric emission from a rough surface is thus definitely indicated.

Viewed with a hand magnifier, the sodium surface looked built up of smooth, polished, round lumps of different sizes forming an almost completely opaque coat over the cathode. The lumps varied in size from approximately 1/10 mm diameter down to smaller than could be seen. No crystalline structure was visible with the hand lens although sodium is known to crystallize in cubic form. The electron optical pictures indicate much the same shape as seen with the hand lens.

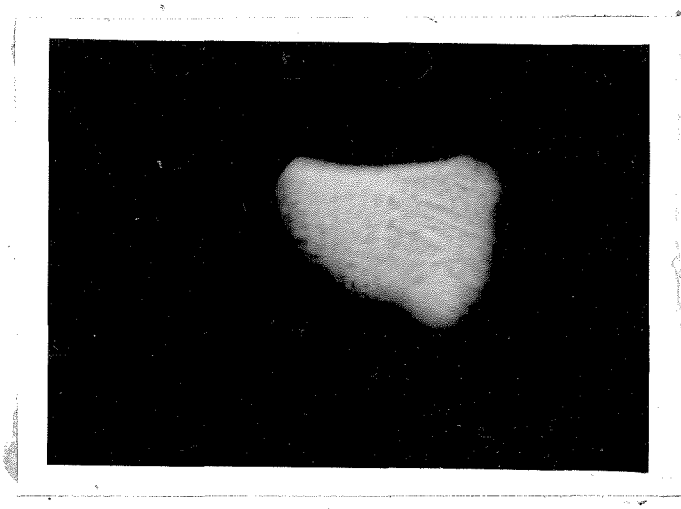

a.

b.

c.

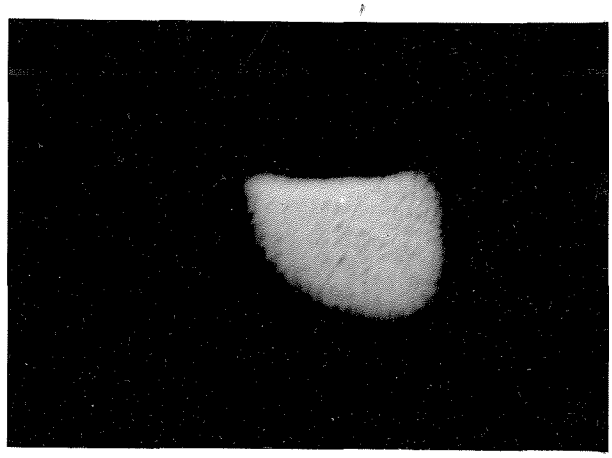

d.

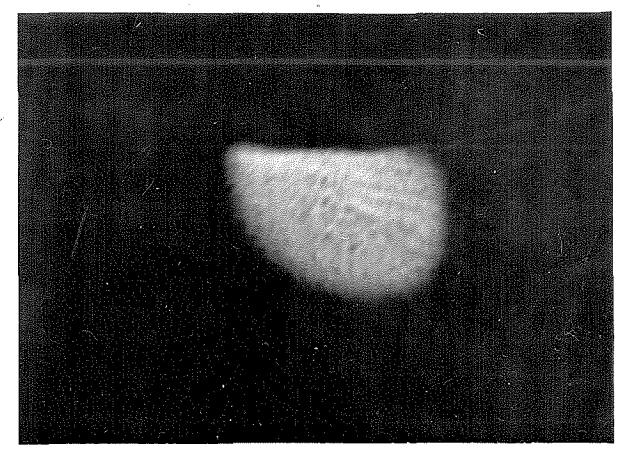

e.

Plate 7.1

7.1 Effect of age on emission

It was thought possible that one would find changes in the emitting area with age of the surface since in photoelectric experiments with sodium the threshold usually shifts during the experiment. Plates 7.1, a - e, are photographs taken over a period of 73 hours beginning with 7-hour old sodium of a cathode illuminated by a mercury arc through a clear plate glass filter. Only a very weak image appeared from light passed by an Eastman 50 blue filter; so that plate glass represented almost entirely emission by light of 3650 A^0 to 4078 A^0. This range was chosen because it gave a high enough emission to photograph while at the same time it was of long enough wave length to probably be above the threshold of any contaminations such as mercury, grease, oxides, or hydroxides. Any gross changes due to contamination should have evidenced themselves by the appearance of new dark spots or by changes in the shape of the existing pattern. The above photographs were checked by superimposing the negatives and by careful comparison with a sterioptican viewer. No difference was seen which could be traced to changes in the emitting surface, although there was a definite difference between the early images and the last ones. The difference in focus probably was sufficient to cause this variation. The same highlights and shadows could be traced throughout the entire set. Pictures 7.1 a and b, the 7-hour and the 13-hour surfaces, which are nearest to the same focus, show no conclusive differences.

Similar sets of pictures were taken over the same 72-hour period using an Eastman 18A filter and using a Vitaglass filter. The pictures were no more conclusive than the ones shown here.

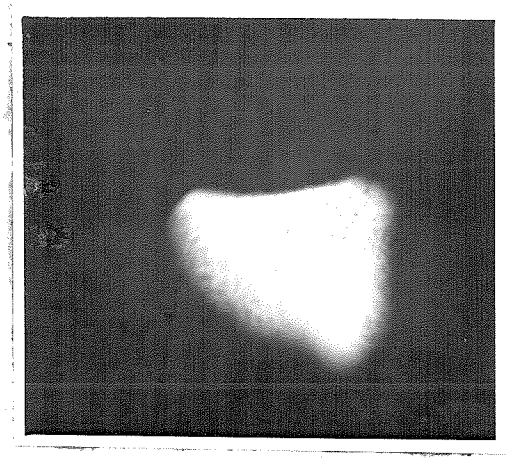

a.

b.

c.

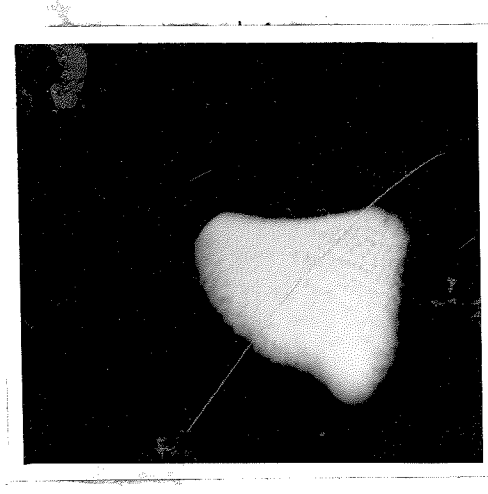

d.

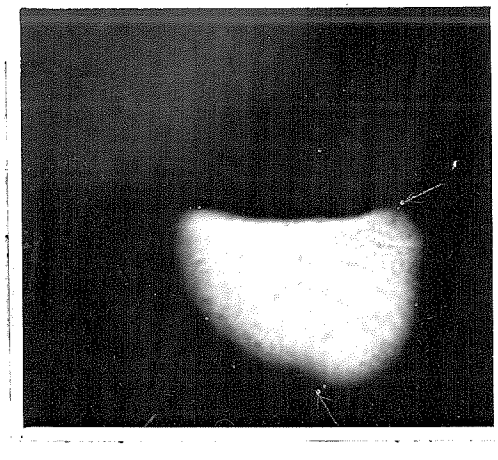

e.

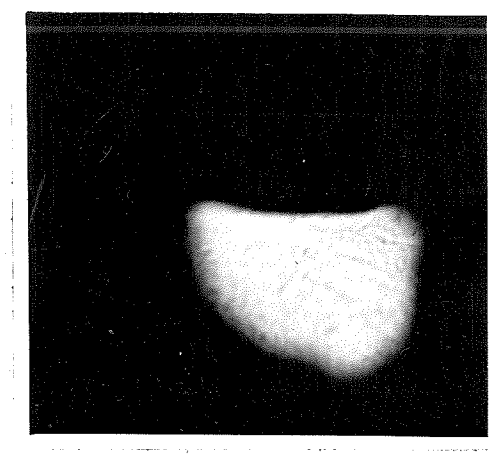

f.

Plate 7.2

Image intensities, as measured by the exposure meter and checked by photographic exposure, did not vary over a period of 6 days; nevertheless, some changes in the sodium surface probably took place although they were small compared with the variations in the focus of the pictures. More reproducible electron accelerating voltage and focal current might show these changes; higher magnification and resolution might be necessary, for the variations may be microscopic. Variations may even be uniform over large areas of surface and hence very difficult to detect; this is conceivably possible since sodium has the viscosity of soft wax and surface tension forces may be very high.

Due to the previously mentioned factors (the quadrant form of the cathode, its lack of smoothness, lack of alignment, and turning of the fluorescent screen) the images were in focus over only a small portion of their area. This area was different for different photographs because of variations in accelerating voltages and focusing currents. However, it seems certain that no changes by factors of 1 part in 4, or probably even 1 part in 10, occured during the experiment in which the photographs were taken.

7.2 Effect of illumination frequency on emission

The photographs 7.2 a-f are a series taken in as rapid a sequence as possible to determine the effect of varying incident wave length of illumination. 7.2 a was taken without filter using the hot mercury arc;

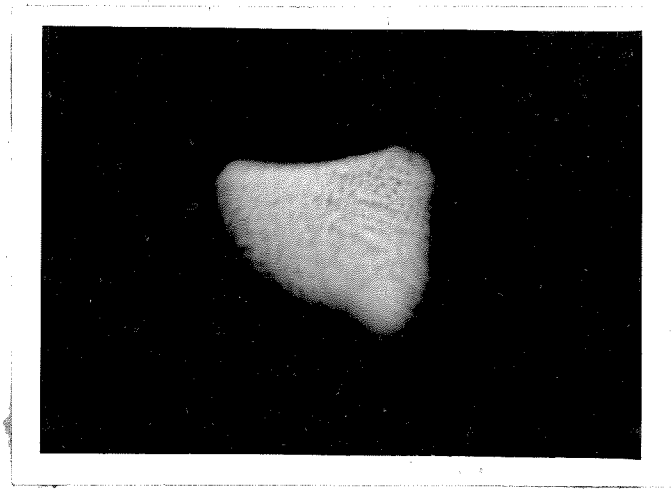

Plate 7.2 a'

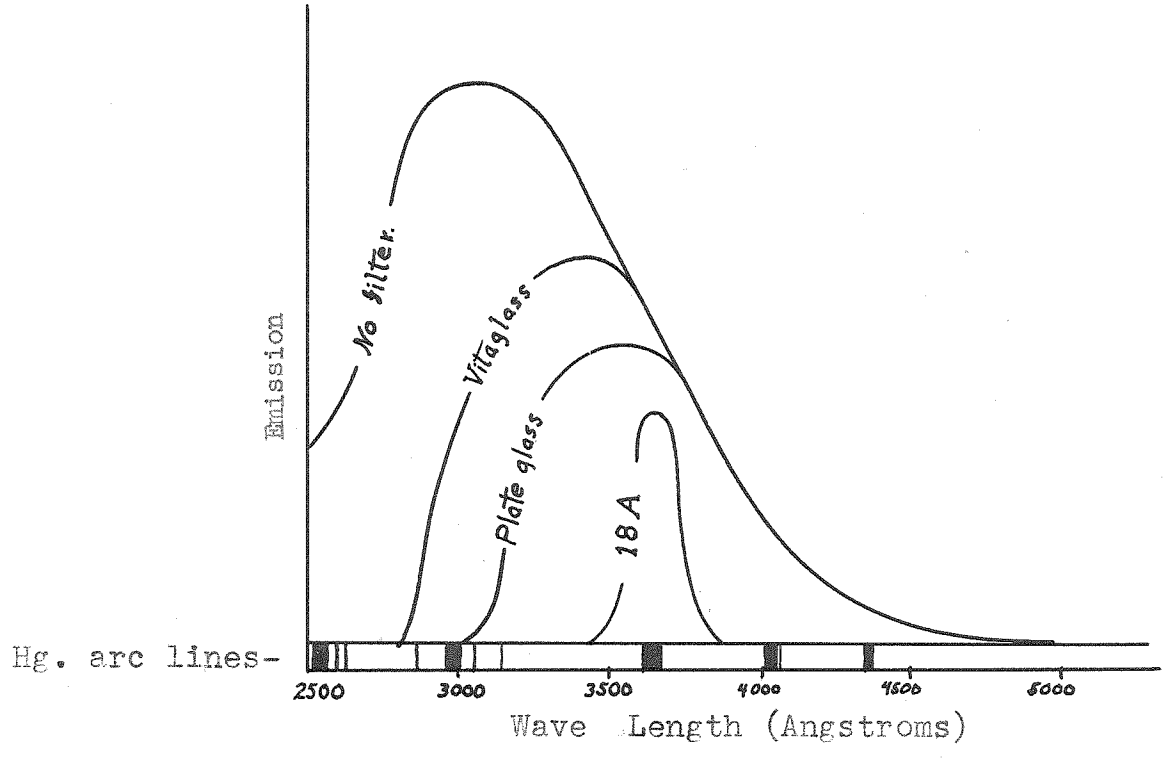

Fig. 7.2 g.

Photoelectric emission of sodium through different filters

a

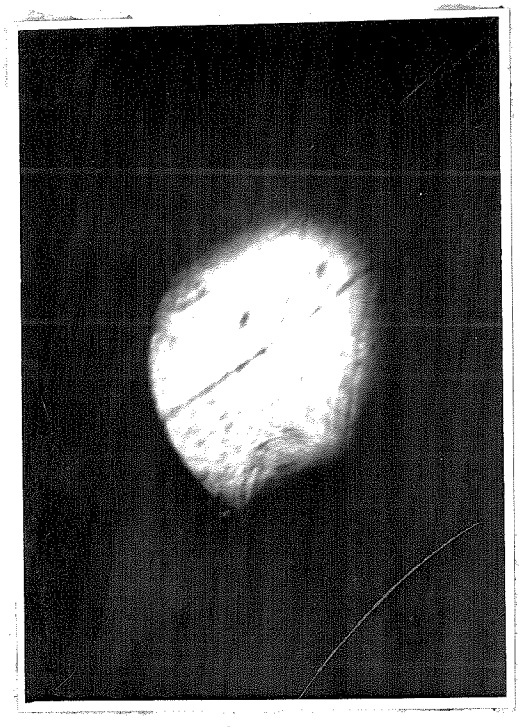

b

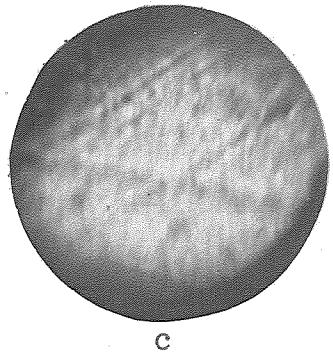

c

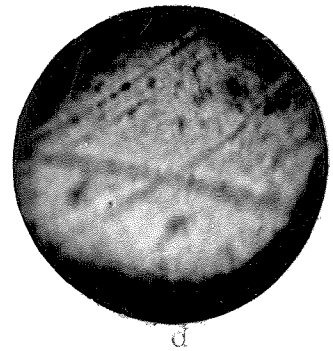

d

Plate 7.3

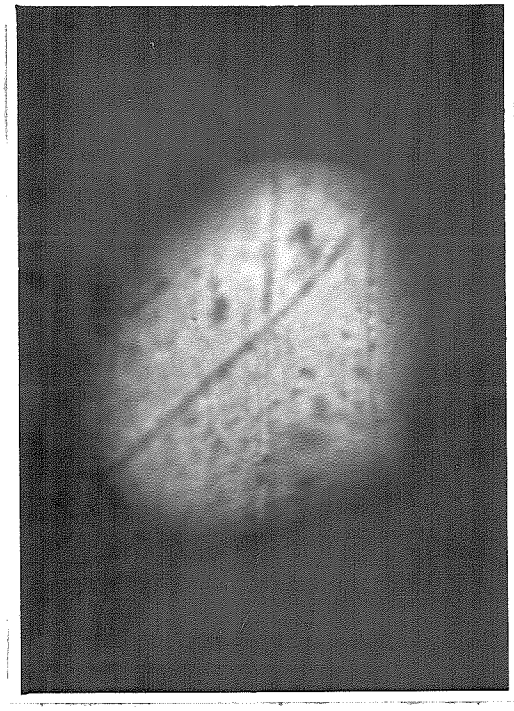

e

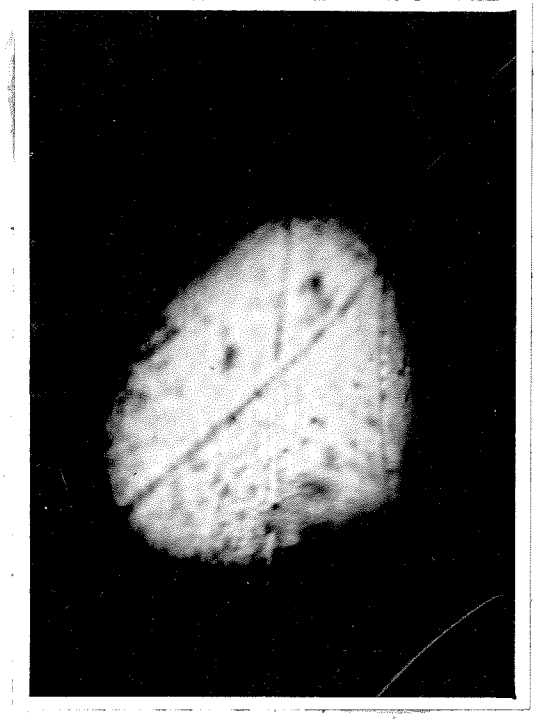

f

g

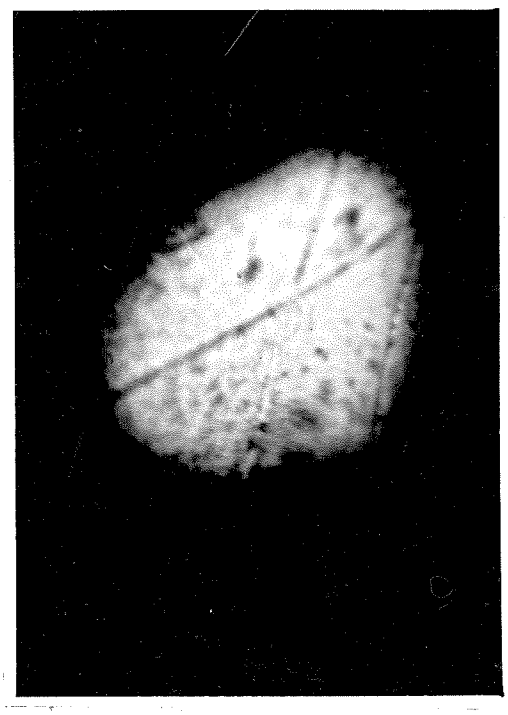

h

Plate 7.3

of emitting area was apparent when the cathode was illuminated by shorter wave lengths although emission was increased 60% by inclusion of energies below 3200 A^{o}. By using a truly flat and scribe-marked cathode, it was possible in this run to obtain images in good focus over a larger area than in the previous runs. Lack of alignment of the cathode, and tilt of the flourescent screen still made it impossible to have the entire field of view in focus at one time.

a. was taken with no filter, and b. with plate glass filter, one half hour after deposition of the sodium surface.

e, f, g, h, were taken in rapid succession one hour after beginning the run. They are, respectively, no filter, plate glass, plate glass, no filter. The mutual consistency of the images is much better than that of plates 7.2. Neither age nor frequency noticeably affected the emission pattern. The run ended after an hour because the magnet developed a short circuit.

c and d were taken without filter at two different angles of illumination, c at approximately 10^{0} to tangential, d at approximately 30^{0}, in order that they might be viewed to give a pseudo-stereoscopic effect showing the scribe marks and sodium lumps. With this in mind they have been trimmed and mounted so that they represent light incident horizontally rather than from the upper corner as in the upper plates.

VIII ACKNOWLEDGMENTS

The writer gratefully expresses his indebtedness to Professor W. V. Houston who instituted this work and guided both the experimental and theorestical parts of it. Much thanks is due also to Professors W. R. Smythe and I. S. Bowen who have given assistance on technical phases of the experiment. Special mention should be made of the valuable discussions which the writer has had with Mr. J. Earl Thomas covering almost all phases of the experiment and theory. To Mr. Thomas and Mr. H. G. Stever also is due thanks for assistance in proofreading and correcting this paper.

REFERENCES

1. C. F. J. Overhage, Phys. Rev., 52, 1039, (1937)

2. R. H. Fowler, Phys. Rev., 38, 45, (1931)

3. L. A. DuBridge, Phys. Rev., 43, 727, (1933)

4. ----------, New Theories of the Photoelectric Effect, Hermann & Cie., Paris (1935)

5. A. G. Hill & L. A. DuBridge, Phys. Rev., 49, 877, (1936)

6. J.J. Brady & V. P. Jacobsmeyer, Phys. Rev., 49, 670, (1936)

7. M. M. Mann & L. A. DuBridge, Phys. Rev., 51, 120, (1937)

8. C. L. Henshaw, Phys. Rev., 52, 854, (1937)

9. J. J. Brady, Phys. Rev., 46, 768, (1934)

10. A.G. Hill & L. A. DuBridge, Phys. Rev., 49, 877, (1936)

11. L.A. DuBridge, Act. Sci. et Ind., 268, (1935)

12. R. J. Cashman & W. S. Huxford, Phys. Rev., 43, 811, (1933)

13. G. R. Wood, Phys. Rev., 44, 353 (1933)

14. W. V. Houston, Phys. Rev., 52, 1047, (1937)

15. K. Mitchell, Proc. Roy. Soc., A146, 442, (1934)

16. ----------, Proc. Camb. Phil. Soc., 31, 416, (1935)

17. W. R. Hamilton, Tran. Roy. Irish Acad., 15, 69, (1828)

18. ----------, Trans. Roy Irish Acad., 16, 3, (1830)

19. ----------, Tran. Roy. Irish Acad., 16, 93, (1830)

20. ----------, Tran. Roy. Irish Acad., 17, 1, (1837)

21. ----------, Abhandhung zur Strahlenoptic, Leipzig, (1833)

22. E. Wiechert, Wied. Ann., 69, 739, (1899)

23. J. A. Fleming, Electrician, Jan. 1.,(1897)

24. F. Braun, Wied. Ann., 60, 522, (1897)

25. W. Westphal, Verh. dtsch. Phys. Ges., 10, 401, (1908)

26. I. G. Maloff & D. W. Epstein, Electron Optics in Television, McGraw Hill, 1938.

27. L. M. Myers, Electron Optics, Van Nostrand,(1939).

28. Frank Gray, Bell Syst. Tech. J., 18, 1 (1939).

29. W. Glaser, Zeit. f.Ph., 115 (1940).

30. O. Scherzer, Abenda, 101, 593, (1936).

31. R. Rebsch, Ann. d. Phys., 31, 551, (1938).

32. O. Scherzer, Zeit. F. Ph., 114, 427, (1939).

33. M.v. Ardenne, Elektron Übermikroskopie, Berlin, (1940).

34. R. Bebsch., Zeit. f. Ph., 116, 729, (1940).

35. D. Gabor, Nature 139, 373, (1937).

36. D. B. Langmuir, Nature 139, 1066, (1937).

37. G. H. Shortley & R. Weller, J. Appl. Ph., 9, 334, (1938).

38. E. Bruche, A.E.G. Mitt., 45, (1934).

39. E. Bruche & H. Johannson, Phys. Zeit., 33, 898, (1933).

40. E. Bruche, Ann. Ph., 15, 145, (1932).

41. M. Knoll & F. G. Houtermans & W. Schulze, Zeit. f. Ph., 78, 340,(1932).

42. E. F. Richter, Zeit. f. Ph., 87, 686, (1934).

43. W. Knecht, Ann.d. Phys., 20, 161, (1934).

44. W. G. Burgers & Ploos van Amstel, Philips Tech. Rev., 1, 312, (1936).

45. R. A. Millikan, Phys. Rev., 7, 18, (1916).

46. I. Tamm & S. Schubin, Zeit. F. Ph., 68, 97,(1931).

47. R. A. Millikan, Phys. Rev., 7, 355, (1916).

48. E. Bruche, Zeit. f. Ph., 86, 448, (1933).

49. J. Pohl, Zeit. f. Tech. Ph., 15, 579, (1934).

50. -------, Phys. Zeit., 35, 1003, (1934).

51. A. Mahl & J. Pohl, Zeit.f. Ph., 16, 219, (1935).

52. M. Knoll & E. Ruska, Ann. d. Phys., 12, 607, (1932).

53. H. W. Leverenz, J.O.S.A., 27, 25, (1937).